FINAL REPORT ON

FURTHER DEVELOPMENT OF A GLOBAL POLLUTION MODEL FOR

CO, CH_4, AND CH_2O
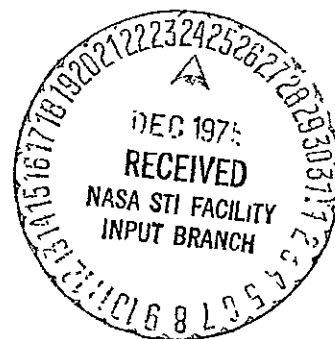
by

Leonard K. Peters
Department of Chemical Engineering
University of Kentucky
Lexington, Kentucky 40506

December 22, 1975

Further Development of·a Global Pollution Model for

CO, CH_4, and CH_2O

FOREWORD

The report is divided into two chapters describing (1) the model
development and description, and (2) the results of long term static
chemical kinetic computer simulations and preliminary short term
dynamic simulations. The work on the dynamic transport/chemistry
model simulations is continuing.

TABLE OF CONTENTS

NOMENCLATURE

c molar concentration of species in the air, kmoles/meter^3

c_ℓ,   molar concentration of species in the absorbing phase, kmoles/meter^3
c_s,
etc.

c^* molar concentration of species in the air if the ocean and air phases were in equilibrium, kmoles/meter^3

C molar density of air, kmoles/meter^3

F molar convective flux, kmoles/meter^2/second

$\mathscr{F}$ molar flux at boundary, kmoles/meter^2/second

J molar diffusive flux, kmoles/meter^2/second

H Henry's Law constant, dimensionless

k reaction rate constant – first order reaction, second^{-1}, second order reaction, meters^3/kmole/second

k_ℓ mass transfer coefficient, meters/second

K absorption coefficient, meter^{-1}

M Molecular weight, kgrams/kmole

$O(\ )$ order of magnitude

p pressure, newtons/meter^2

r radial coordinate position, meters

R ideal gas law constant, 8.314×10^3 joules/kmole/°K

R molar species generation by chemical reaction, kmoles/meter^3/second

S species source at boundary, kmoles/meter^2/second

t time, seconds

T temperature, °K

u velocity in the ϕ-direction, meters/second

v velocity in the θ-direction, meters/second

w velocity in the r-direction, meters/second

x mole fraction (volumetric mixing ratio) of methane, dimensionless

y mole fraction (volumetric mixing ratio) of formaldehyde, dimensionless

z mole fraction (volumetric mixing ratio) of carbon monoxide, dimensionless

α_1 dimensionless constant, Equation (50)

α_2 dimensionless constant, Equation (51)

$\Delta-$ incremental change in variable

Δ representative grid interval, meters

ε turbulent eddy diffusivity, $\text{meters}^2/\text{second}$

ε_0 kinetic energy dissipation rate, $\text{meters}^2/\text{second}^3$

θ coordinate position relative to equator, degrees

ϕ coordinate position, degrees

ω vorticity, second^{-1}

Subscripts

G ground level

i grid point in ϕ-coordinate

j grid point in θ-coordinate

k grid point in r-coordinate

ℓ absorbing phase

P pollutant

PS pollutant soil product

S soil

T tropopause

Superscripts

n	time level
r	r-direction
v	volumetric averaged
x	methane
y	formaldehyde
z	carbon monoxide
θ	θ-direction
φ	φ-direction
−	grid scale averaging operator

CHAPTER 1

MODEL DEVELOPMENT AND DESCRIPTION

Transport/chemistry models that describe the circulation of a species
in the atmosphere can be extremely beneficial in understanding the physical
and chemical processes occurring between the sources and sinks of a pol-
lutant. In this chapter, such a model for the methane-carbon monoxide
system is discussed. The model considers the physico-chemical action of
these pollutants in the troposphere. This restriction is convenient
since the tropopause provides a natural boundary across which little
transport occurs. The data on sources and sinks for these pollutants
is discussed, and the estimates of these strengths are based on the best
available information relative to the major anthropogenic and natural
contributions. The incorporation of the source-sink descriptions into
the model is discussed in detail.

The distribution and concentrations of methane and carbon monoxide
in the atmosphere are interrelated by the chemical reactions in which
they participate. A chemical kinetic model based on the pseudo-steady
state approximation for the intermediate species and for inclusion in
the species continuity equation was developed to account for these
reactions. Therefore, mass conservation equations are only required
for the methane and carbon monoxide.

The numerical procedure employed to mathematically describe the
transport/chemistry is a mass conservative scheme employing an integral
flux approach. It is fourth-order accurate in space which is desirable

2

in simulating convective processes in three space dimensions. Since computer storage places restrictions on the scale of transport processes that are explicity calculated, smaller scale mixing is described using an artificial diffusivity. This is analogous to the concept of the artificial viscosity which is useful in the global circulation models. The results of the computer simulations using this model will be discussed in the next chapter.

INTRODUCTION

Global transport/chemistry models of pollutants can be employed to analyze the circulation of pollution from its sources to sinks. Furthermore, these models can be significant in placing anthropogenic sources in proper perspective on a global scale. In this chapter and the subsequent chapter, the development and the computer simulation results of a tropospheric global model for methane (CH_4) and carbon monoxide (CO) are presented.

The analysis is accomplished by geographically distributing the sources and sinks of CO, CH_4, and CH_2O, and simulating their convective and diffusive transport by numerical solution on the computer of the three dimensional turbulent diffusion equation. The atmospheric phenomena of these species are coupled through atmospheric chemical reactions that occur. Thus, the species must be considered simultaneously. Generally speaking, the oxidation of methane produces formaldehyde which decomposes to carbon monoxide. Other sources and

sinks of these pollutants are, of course, operating.

Most analyses to the present have utilized a global residence time approach[cf., 1,2,3,4,5]. Models incorporating a multiplicity of sources and sinks have not generally been attempted. The model that is described employs known source and sink strength data, the atmospheric chemistry of the pollutants in question, monthly averaged climatological data, and the turbulent diffusion equation for CH_4 and CO to establish global concentration distributions.

PHYSICO-CHEMICAL CONSIDERATIONS

The model development is restricted to the troposphere. This is a logical boundary since the tropopause provides a natural surface thru which the rate of mass transfer is relatively low. Furthermore, the photolytic decomposition of CO_2 appears to be unimportant as a source of CO in the troposphere[6], and this enables one to decouple the CO transport from the CO_2 transport. The sources and sinks of methane, formaldehyde, and carbon monoxide will be briefly reviewed to provide a better appreciation of this complex system. Figure 1 illustrates the principal interactions that occur.

Sources and Sinks of CH_4

The sources and sinks of methane appear to be reasonably well understood at the present. The anthropogenic sources are largely the result of internal combustion engines and oil drilling and refinery operations. These emissions can be fairly well mapped based on automobile density and industrial activities.
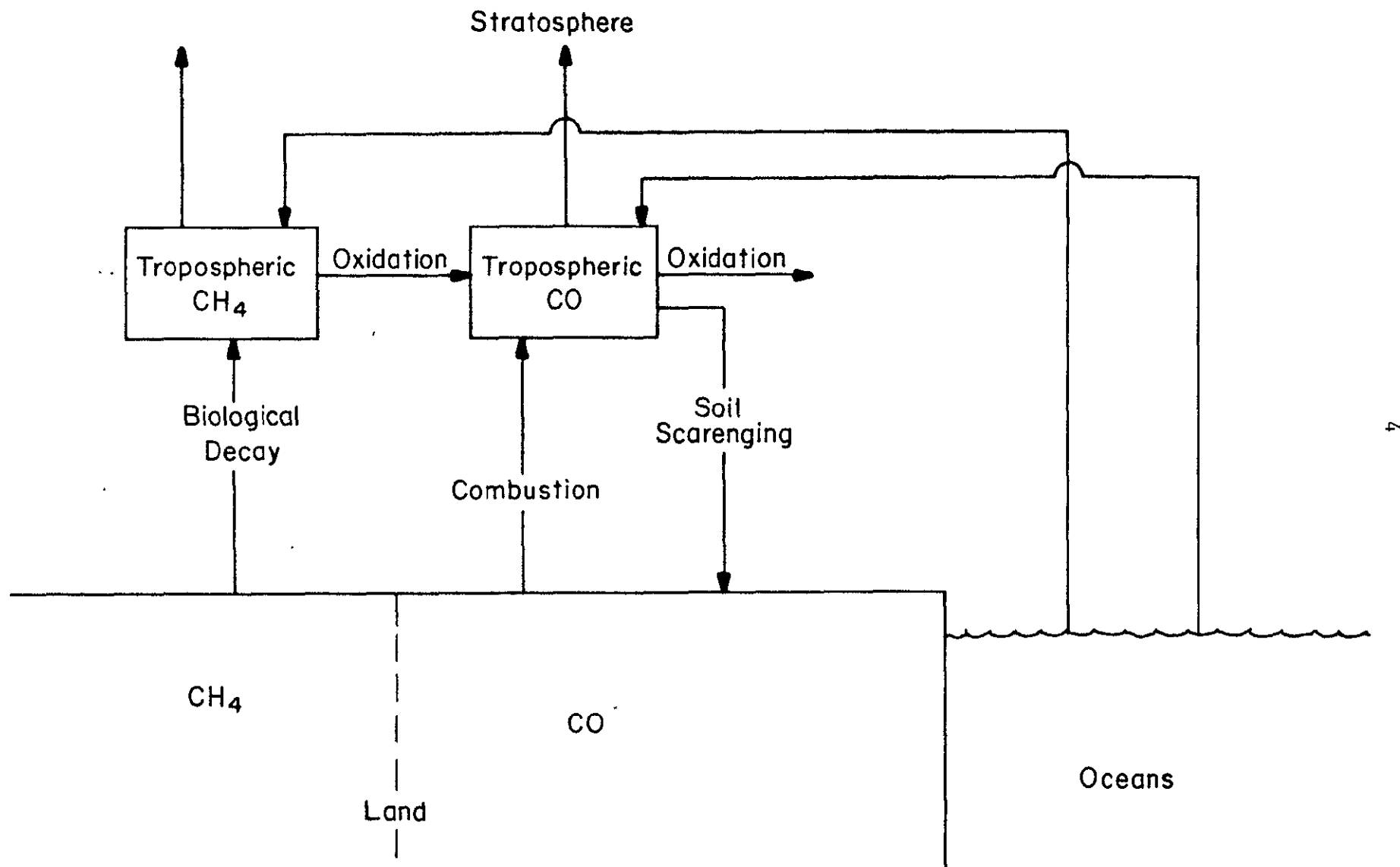
Figure 1

Schematic of the Methane-Carbon Monoxide Interactions

The natural sources apparently far out strip the man made sources –
the principal ones being decaying vegetation and other biological action.
Some of this biological action occurs within marine environments, and
as a result the surface waters of the oceans, bays, and rivers appear
to be supersaturated with methane. Lamontagne, Swinnerton, Linnenbom,
and Smith[7] have reported equivalent surface ocean and sea water
concentrations about 1.2 to 1.7 times the corresponding atmospheric
concentrations. Specifically in open tropical ocean waters, the surface
concentrations (4.7×10^{-5} ml/l) corresponded to an equilibrium atmos-
pheric concentration of 1.80 ppm, whereas the measured atmospheric con-
centrations averaged 1.38 ppm. Bay and river waters appear to be even
more heavily supersaturated. Their results specifically cited the
following supersaturation ratios: Chesapeake Bay – 14.3, York River –
21.2, Mississippi River – 5.67, Potomac River – 36.0. These values
may also be affected by local pollution problems. The data of Brooks
and Sackett[8] on the coastal waters of the Gulf of Mexico generally
support Lamontagne et al's results. However, they report that in the
Yucutan area, where there is a major upwelling of deep water with low
hydrocarbon concentration, the Gulf of Mexico acts as a sink for
methane.

The principal sink mechanism for methane appears to be in the
homogeneous gas phase reaction of methane with hydroxyl radicals.

$$CH_4 + OH \rightarrow CH_3 + H_2O \qquad\qquad (1)$$

The methyl radical can subsequently undergo reactions which result in formaldehyde and ultimately in CO formation. Thus, this sink for methane provides one natural source for formaldehyde and carbon monoxide. The following sequence of reactions is responsible for producing the hydroxyl radical[2].

$$O_3 + h\nu \rightarrow O(^1D) + O_2 \tag{2}$$

$$O(^1D) + H_2O \rightarrow 2OH \tag{3}$$

$$O(^1D) + M \rightarrow O + M \tag{4}$$

$$O + O_2 + M \rightarrow O_3 + M \tag{5}$$
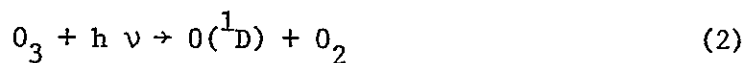
It will be noted later that the hydroxyl and atomic oxygen (O) are also important in reactions with CO.

Sources and Sinks of CH_2O

The anthropogenic sources of formaldehyde appear to be relatively small - the main ones being direct emission from automobile exhaust and formation during photochemical smog episodes. These estimates can be fairly reliably based on past auto exhaust emission estimates and studies.

The only apparent natural source for CH_2O is from the methane oxidation just cited. Levy[9,10] and McConnell, McElroy, and Wofsy[11] have suggested the following steps in the formation of formaldehyde by this mechanism.

$$CH_4 + OH \rightarrow CH_3 + H_2O \tag{1}$$

$$CH_3 + O_2 + M \rightarrow CH_3O_2 + M \qquad\qquad (6)$$

$$CH_3O_2 + NO \rightarrow CH_3O + NO_2 \qquad\qquad (7)$$

$$CH_3O_2 + CH_3O_2 \rightarrow 2CH_3O + O_2 \qquad\qquad (8)$$

$$CH_3O + O_2 \rightarrow CH_2O + HO_2 \qquad\qquad (9)$$
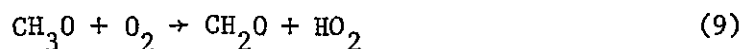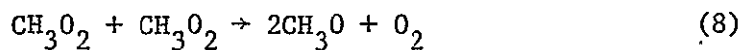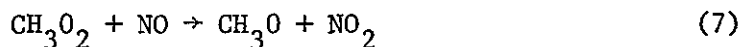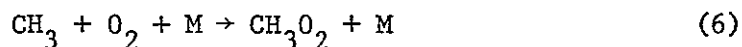
Thus, the formaldehyde formation and concentration is directly coupled to the methane distribution.

The main sink for formaldehyde is in the photochemical decomposition and reaction with hydroxyl radicals. The following reactions appear to be importort[9,10,11].

$$CH_2O + h\nu \rightarrow CHO + H \qquad\qquad (10)$$

$$CH_2O + h\nu \rightarrow H_2 + CO \qquad\qquad (11)$$

$$CH_2O + OH \rightarrow CHO + H_2O \qquad\qquad (12)$$

The production of CHO also leads to carbon monoxide formation via[13,14]

$$CHO + O_2 \rightarrow CO + HO_2 \qquad\qquad (13).$$

Therefore, the source and sink distribution of formaldehyde is primarily due to homogeneous gas phase reactions and is coupled to the methane and carbon monoxide distributions.

Sources and Sinks of CO

Bortner, Kummler, and Jaffe[2] and, more recently, Seiler[12] have summarized the sources, sinks, and concentrations of carbon monoxide. A very significant feature of the global distribution of CO is the difference of the mixing ratios found in the Northern and Southern Hemispheres. North of the intertropical convergence zone typical concentrations over oceans are 0.15 ppm - 0.20 ppm, whereas south of the intertropical convergence zone the CO mixing ratios drop rather rapidly to 0.08 ppm. Seiler[12] has summarized most of the data on which these results are based, and he suggests average tropospheric concentrations of 0.15 ppm and 0.08 ppm in the Northern and Southern Hemispheres, respectivly.

The world-wide anthropogenic sources are estimated to be in excess of 300 million tons/year with two-thirds or more resulting from motor vehicle emissions. The remainder is distributed between stationary combustion sources, industrial processing, and incineration. Therefore, these sources are distributed largely according to motor vehicle density.

The major natural sources of carbon monoxide appear to be the oceans, forest fires, terpene photochemistry, and gas phase reactions. The studies of Junge, Seiler, and Warneck[4], Seiler and Junge[13], Swinnerton, Linnenbom, and Check[14], Lamontagne, Swinnerton, and Linnenbom[15] and Swinnerton and Lamontagne[16] indicate that the level of excess CO in the ocean corresponds to an equilibrium air phase concentration of about 3.5 ppm. These data were obtained during ocean cruises. The recent data of Meadows and Spedding[17], however, suggest

9

that the degree of supersaturation may not be nearly as large. The

previously mentioned studies based their calculations on CO solubility

obtained for pure CO in the gas phase at pressures greater than or equal

to one atmosphere. Meadows and Spedding, on the other hand, conducted

experiments in distilled water and seawater where the gas phase CO con-

centration was in the 3 ppm - 18 ppm range and found the solubilities to

be more than eight times as high. These data would suggest that the

oceanic source strength is not nearly as large as the other workers

have suggested and that the equilibrium air phase concentration may

be more like 0.3 ppm to 0.4 ppm rather than 3.5 ppm.

It is, of course, reasonable to expect that the river, lake, or

ocean regions near urban areas, where the atmospheric CO concentrations

may be considerably larger than 3.5 ppm, may act as a sink for CO.

Furthermore, it is possible that the oceans at the high latitudes serve

as a sink for CO produced by oceans at the low latitudes. This would be

expected since the warmer tropical waters would likely have a higher

biological activity producing more CO. With the warmer water, the

solubility of CO is reduced. Transport over colder waters with greater

CO solubility capacity would create the possibility of these sections

acting as a sink for CO. Thus, it is plausible that the oceans act

as both a source and sink for CO. Similar arguments could be made

for methane.

In addition to terpene photochemistry and forest fires (combined

sources are estimated at 23 x 10^6 ton/year[18]), another principal

natural source of CO appears to be the gas phase reactions cited

earlier. The estimate of the gas phase oxidation of CH_4 to CO is directly related to the hydroxyl concentration. Since there have been no direct measurements made of the hydroxyl radical concentration, there is considerable uncertainty as to the magnitude of this source of CO. Various estimates place this anywhere up to ten times the anthropogenic source[12,19]. However, the relatively slow inter-hemispheric transport[20] from the north to south and the substantial differences in the CO concentration between the two hemispheres would suggest much lower estimates since the gas phase oxidation would not be favored in either hemisphere. The reactions forming CO cannot be divorced from the reactions which consume CO, of which the following seem to be important[2].

$$CO + OH \rightarrow CO_2 + H \tag{14}$$

$$CO + O + M \rightarrow CO_2 + M \tag{15}$$

$$CO + N_2O \xrightarrow{Surface} CO_2 + N_2 \tag{16}$$

$$CO + HO_2 \rightarrow CO_2 + OH \tag{17}$$
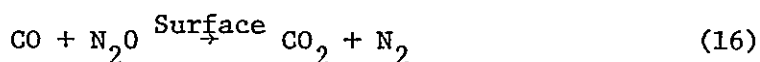
Reaction (16)[21,22,23,24,25] is reportedly first order in CO but zeroth order in N_2O. This is a surface catalyzed reaction and would require, for complete accuracy, detailed information on the atmospheric aerosol as to size distribution and chemical composition. Since these data are very scarce, there is considerable uncertainty in employing Reaction (16) in any model.

Reaction (17) has been suggested by Westenberg[26] to be important

in atmospheric pollution problems. However, the results of Davis, Wong,

Payne, and Stief[27] indicate that it is unimportant in the overall

oxidation processes of CO. As a result, the present model development

ignores Reaction(17).

Another natural sink of CO of seemingly large significance is the

soil. The work of Inman[28], Liebl[29], Inman, Ingersoll, and Levy[30],

Ingersoll and Inman[31], and Ingersoll, Inman , and Fisher[32], point

up this significance. The field studies of Inman, Ingersoll and co-

workers exposed soils in situ and in the laboratory to test atmospheres

containing 100 ppm of CO. These showed average uptake rates that varied

from 1.1 mg CO/hr m^2 to 64.5 mg CO/hr m^2. On the low end were soils

under cultivation and desert areas, and on the high end were tropical

deciduous forest areas and soils near roadways. By using an average

concentration driving force of 50 ppm CO and assuming conditions of

atmospheric pressure and 20°C, the mass transfer coefficient at the

surface corresponds to 5.27×10^{-6} m/sec and 3.09×10^{-4} m/sec,

respectively. The data of Liebl[29] were obtained at

more realistic CO mixing ratios — on the order of 0.25 ppm — than that

of Inman, Ingersoll and co-workers. Liebl also showed uptake of CO by

the soils. In addition, he showed a CO production capability when the

air above the soil was initially free of any CO. These data indicate,

as Seiler and Junge[13] have suggested, that at low concentrations

(around 0.2 ppm at 25°C) a temperature dependent equilibrium of CO above

soils occurs. However, for soil temperatures below 20°C, the CO mixing

ratio continued to decrease to a value lower than 2 ppb. If this is

truly the case, then the soils can act as either sinks or sources for carbon monoxide in much the same manner as do the oceans. Evaluation of exchange coefficients based on Liebl's data indicates a value an order of magnitude or so larger. However, this may simply be indicative of soil difference since he used soil obtained from a greenhouse.

These scattered values are probably indicative of the rate of the biological reaction that is occurring near the surface of the soil and may simply be representative of the type and concentration of the soil micro-organisms utilizing CO. One of the big uncertainities relative to soil scavenging is the determination of which fraction of these micro-organisms are anaerobic methane-producing[33] and what fraction are aerobic CO_2 producing.

A source and/or sink common to all three species is leakage from and/or to the stratosphere. Since the initial model is restricted to the troposphere, this leakage must be considered as sources and/or sinks. In the specific case of CO, leakage from the troposphere to the stratosphere is reasonable to expect since the CO that escapes thru the tropopause will typcially undergo chemical reactions and not return to the troposphere as CO. This is substantiated by the vertical profiles of CO which show a decrease of CO mixing ratio with height above the tropopause[34]. The leakage of CH_4 thru the tropopause appears to be similar to that for CO since vertical profiles of CH_4 also show a decrease with increasing altitude above the tropopause[35,36].

MATHEMATICAL MODEL

The transport of a gaseous compound in the atmosphere is mathematically described by the species continuity equation with the inclusion of any homogeneous generation or loss terms. By distributing the sources and sinks of the various species on the Earth's surface and at the tropopause consistent with the physico-chemical considerations, the appropriate boundary conditions can be incorporated into the solution.

Mathematical Overview

The diffusion equation written in spherical coordinates using the turbulent eddy diffusivity concept is

$$\frac{\partial x_A}{\partial t} + w \frac{\partial x_A}{\partial r} + \frac{v}{r} \frac{\partial x_A}{\partial \theta} + \frac{u}{r \cos \theta} \frac{\partial x_A}{\partial \phi} =$$

$$\frac{\varepsilon}{C} \left[\frac{1}{r^2} \frac{\partial}{\partial r} \left(r^2 C \frac{\partial x_A}{\partial r} \right) + \frac{1}{r^2 \cos \theta} \frac{\partial}{\partial \theta} \left(\cos \theta \, C \frac{\partial x_A}{\partial \theta} \right) \right.$$

$$\left. + \frac{1}{r^2 \cos^2 \theta} \frac{\partial}{\partial \phi} \left(C \frac{\partial x_A}{\partial \phi} \right) \right] + \frac{1}{C} (R_A + \hat{R}_A) \qquad (18).$$

In Equation (18) the eddy diffusivity has been assumed constant, and x_A is the mole fraction of species A, expressible as ppm by volume if so desired; C is the molar density, which for air can be determined by using the ideal gas law ($C = \frac{p}{RT}$); R_A is the generation or loss of species A by chemical reaction; and $\hat{R}_A$ is a term which accounts for the effects of turbulence on the chemical reaction[37]. The latter term arises
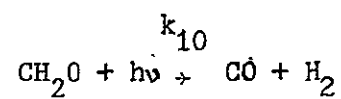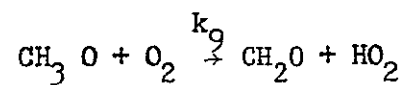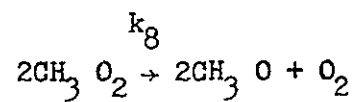
from turbulent fluctuations in the species concentrations. For a single

first order chemical reaction $\hat{R}_A'$ is zero, but for more complex chemical

kinetics this term is not zero. However, in many cases this term is

relatively unimportant and in the future development, $\hat{R}_A$ will be con-

sidered to be zero.

Due to the well known closure problem caused by the introduction of

fluctuating quantities, one is usually forced to parameterize the turbulent

quantities. Perhaps the easiest and most commonly used procedure to solve

the closure problem is to introduce the eddy diffusivity as has been done

in Equation (18). There is one problem that should be recognized with

the use of the eddy diffusivity. Since the time scale associated with

atmospheric motion can be quite large, unlike that in the more frequently

encountered boundary layer flows, the duration of time averaging must

generally be relatively long to include all fluctuations. In fact, this

length of time is prohibitively long, and one must be satisfied with

averaging times that are short in comparison. As a result, the eddy

diffusivities that are used must be consistent with this concept and

are directly dependent upon the time and length scale of the averaging.

As Equation (18) now stands, numerical solution is required.

However, it is further complicated by the highly non-linear character

of the generation term. The problems associated with the numerical

solution are discussed in the next section.

Chemical Reaction Model

Based on the considerations presented previously, the following reaction sequence currently seems plausible to describe the generation terms.

$$O_3 + h\nu \xrightarrow{k_1} O(^1D) + O_2$$

$$O(^1D) + H_2O \xrightarrow{k_2} 2\ OH$$

$$O(^1D) + M_3 \xrightarrow{k_3} O + M_3$$

$$O + O_2 + M_4 \xrightarrow{k_4} O_3 + M_4$$

$$CH_4 + OH \xrightarrow{k_5} CH_3 + H_2O$$

$$CH_3 + O_2 + M_6 \xrightarrow{k_6} CH_3\ O_2 + M_6$$

$$CH_3\ O_2 + NO \xrightarrow{k_7} CH_3\ O + NO_2$$

$$2CH_3\ O_2 \xrightarrow{k_8} 2CH_3\ O + O_2$$

$$CH_3\ O + O_2 \xrightarrow{k_9} CH_2O + HO_2$$

$$CH_2O + h\nu \xrightarrow{k_{10}} CO + H_2$$

$$CH_2O + h\nu \xrightarrow{k_{11}} CHO + H$$

$$CH_2O + OH \xrightarrow{k_{12}} CHO + H_2O$$

$$CHO + O_2 \xrightarrow{k_{13}} CO + HO_2$$

$$CO + O + M_{14} \xrightarrow{k_{14}} CO_2 + M_{14}$$

$$CO + OH \xrightarrow{k_{15}} CO_2 + H$$

$$CO + N_2O \xrightarrow[Surface]{k_{16}} CO_2 + N_2$$
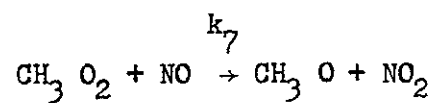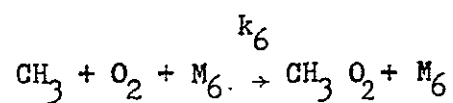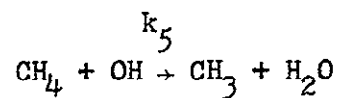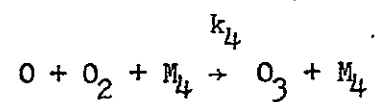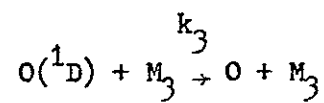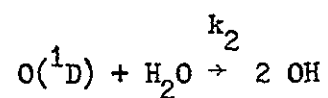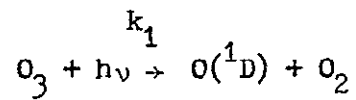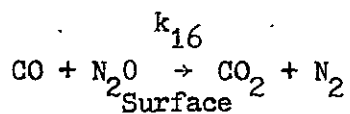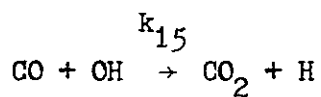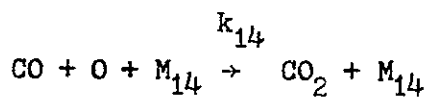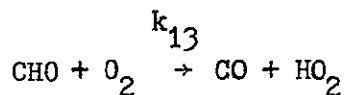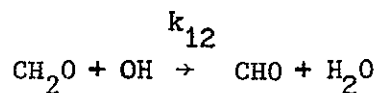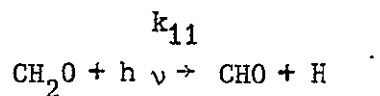
By considering this mechanism, the generation term for methane can be written as

$$R_{CH_4} = -k_5 c_{CH_4} c_{OH} \tag{19},$$

and for CH_2O it becomes

$$R_{CH_2O} = k_9 c_{CH_3O} c_{O_2} - (k_{10} + k_{11}) c_{CH_2O}$$

$$- k_{12} c_{CH_2O} c_{OH} \tag{20}.$$

Finally, the generation term for CO is

$$R_{CO} = k_{10} c_{CH_2O} + k_{13} c_{CHO} c_{O_2} - k_{14} c_{CO} c_O c_{M_{14}}$$

$$- k_{15} c_{CO} c_{OH} - k_{16} c_{CO} \tag{21}.$$

In order to evaluate Equations (19) thru (21), it is necessary to know the concentrations of the various radical species involved. The pseudo-steady state approximation can be used to obtain these estimates. Let us digress momentarily and discuss the pseudo-steady state approximation since it has only been infrequently used for geochemical problems. If one considers the reaction sequence to be occurring in a static system, the set of ordinary differential equations that describes the chemical kinetics is representative of a stiff system. A system of differential equations is said to be stiff if the characteristic time constants of the individual steps vary greatly, i.e., the rate constants are substantially different. Such is the case with the current system. Characteristic of the solution behavior of these systems is a very rapid initial change in some variables (these are said to be the stiff variables) followed by a slowly varying state. Over this time period, the non-stiff variables may change little or not at all.

The numerical solution of stiff systems presents great computational difficulties, and a substantial literature (c.f., Reference (38) as a recent summation of the state of the art) has been developed around their solution. For absolute numerical stability of the system, most integration schemes require that the time step be less than the smallest characteristic time constant. Numerical integration schemes such as the Gear package[39] are attempts at circumventing this problem.

The pseudo-steady state approximation is another way of circumventing this problem if the variables of interest are the non-stiff ones. For the

current situation, this is true since our principal interests are with CH_4 and CO. By exploiting the pseudo-steady state approximation, we can reduce a stiff system to a non-stiff system with little change in the accuracy of the non-stiff variables. As an aside, Lapidus, Aiken, and Liu[40] have shown that the pseudo-steady state approximation can actually improve the accuracy in certain very stiff systems where the computation time, by practical considerations, limits the smallness of the integration time step.

The intermediate species, or stiff variables, exist in very low concentrations due to their high reactivity. As such they adjust to perturbations in the concentrations of CH_4, CH_2O, or CO very rapidly. These transients only last for fractions of a second (on the order of 10^{-5} seconds and smaller) and the pseudo-steady state approximation is thus valid for time scales larger than this. This will be discussed in more detail later.

Using the pseudo-steady state approximation and assuming that the concentrations of H_2O, O_3, and the third bodies (M_3, M_4, M_{14}) can be reliably specified, the results are

$$R_{CH_4} = - \frac{2k_1 k_2 k_5 c_{H_2O} c_{O_3} c_{CH_4}}{(k_5 c_{CH_4} + k_{12} c_{CH_2O} + k_{15} c_{CO}) (k_2 c_{H_2O} + k_3 c_{M_3})} \qquad (22),$$

$$R_{CH_2O} = \frac{2k_1 k_2 c_{H_2O} c_{O_3} (k_5 c_{CH_4} - k_{12} c_{CH_2O})}{(k_5 c_{CH_4} + k_{12} c_{CH_2O} + k_{15} c_{CO}) (k_2 c_{H_2O} + k_3 c_{M_3})}$$

$$- (k_{10} + k_{11}) c_{CH_2O} \qquad (23),$$

and

$$R_{CO} = (k_{10} + k_{11})c_{CH_2O} + \frac{2k_1k_2c_{H_2O}c_{O_3} \; (k_{12}c_{CH_2O} - k_{15}c_{CO})}{(k_5c_{CH_4} + k_{12}c_{CH_2O} + k_{15}c_{CO}) \; (k_2c_{H_2O} + k_3c_{M_3})}$$

$$- \frac{k_1k_3k_{14}c_{O_3} \; c_{M_3} \; c_{M_{14}} \; c_{CO}}{(k_2c_{H_2O} + k_3 \; c_{M_3}) \; (k_4c_{O_2} \; c_{M_4} + k_{14} \; c_{CO} \; c_{M_{14}})} \; -k_{16}c_{CO} \quad (24).$$

Interaction with Oceans

In solving the turbulent diffusion equation, the boundary condition establishes whether the surface acts as a source or sink, or is passive to the transport process. This boundary condition is written as

$$- \varepsilon_r \left. \frac{\partial c}{\partial r} \right|_{r=R} = k_\ell (c_{\ell_b} - c_\ell \big|_{r=R}) \quad (25).$$

In Equation (25), c is the air phase concentration of the species, c_{ℓ_b} is the bulk concentration of the species in the ocean phase, $c_\ell \big|_{r=R}$ is the concentration on the ocean phase side of the interface, and k_ℓ is the ocean phase turbulent exchange coefficient. For sufficiently dilute systems, Henry's Law can be used to relate gas phase and liquid phase concentrations at the interface. If H is Henry's Law constant, then for equilibrium at the ocean-air interface

$$c \big|_{r=R} = H \; c_\ell \big|_{r=R} \quad (26).$$

Thus the boundary condition is written as

$$\frac{\partial c}{\partial r}\bigg|_{r=R} = \frac{k_\ell}{\varepsilon_r H} \left(c\big|_{r=R} - c_\ell^* \right) \tag{27},$$

where c_ℓ^* represents the air phase concentration if the ocean and air were in equilibrium; i.e.,

$$c_\ell^* = H \, c_{\ell_b} \tag{28}.$$

From this point the absorption coefficient, K_ℓ, is used for convenience.

$$K_\ell = \frac{k_\ell}{\varepsilon_r H} \tag{29}$$

Absorption (ocean operating as a sink) would be determined by $c\big|_{r=R} > c_\ell^*$, and desorption (ocean operating as a source) would be determined by $c\big|_{r=R} < c_\ell^*$.

The estimation of K_ℓ presents some difficulties and uncertainties. Henry's Law constant may be the least uncertain quantity and is known fairly accurately for distribution between air and fresh water. H depends on the water temperature and generally increases for increasing water temperature. Obviously this effect must be taken into account. Less certain is the estimate of k_ℓ. Okubo[41] presents representative values of the vertical oceanic eddy diffusivity in the Cape Kennedy area to be 1.3 cm^2/sec to 10 cm^2/sec. If the film model for mass

trasnfer is used to estimate k_ℓ and if the film thickness is assumed to be the 70 meter thick upper-ocean layer, then using the mid-range that Okubo has cited (i.e., 10 cm^2/sec)

$$k_\ell = \frac{10 \ cm^2/sec}{70 \ m} = 1.43 \times 10^{-5} \ m/sec \qquad (30).$$

This value of k_ℓ agrees reasonably well with values estimated from Broecker, Li, and Peng's[42] report of the CO_2 flux ($k_\ell = 3.31 \times 10^{-5}$ m/sec) and Junge, Seiler, and Warneck's[4] estimate of the oceanic CO source strength ($k_\ell = 0.410 \times 10^{-5}$ m/sec). Values of ε_r which must be based on the grid mesh size in order to realistically simulate the subgrid scale mixing processes will be discussed later.

As long as H and c_ℓ^* are known for the particular species, the boundary condition then accounts for the operation of the ocean as a source or a sink. For example, c_ℓ^* for CO appears to be around 3.5 ppm (although the results of Meadows and Spedding[17] indicate a possibly much lower value) and for CH_4 it is around 1.8 ppm.

Interaction with Soils

Interaction with soils is a combination of physical, chemical, and biological actions. However, if one assumes a very simple scheme of a general pollutant P interacting with the soil S, a result analogous to that for the oceans is obtained. For example, consider

$$P + S \xrightarrow{k'_s} PS \qquad (31)$$

$$PS \xrightarrow{k''_s} P + S \qquad (32).$$

Then

$$-\varepsilon_r \left. \frac{\partial c_P}{\partial r} \right|_{r=R} = k_s'' \, c_{PS} - k_s' \, c_S c_P \qquad (33).$$

If c_S and c_{PS} are relatively constant and in large excess one obtains

$$-\varepsilon_r \left. \frac{\partial c_P}{\partial r} \right|_{r=R} = k_s \, (c_S^* - c_P) \qquad (34),$$

where c_S^* is the equilibrium concentration. This is the quantity to which Seiler and Junge[13] ascribe the value of about 0.2 ppm at 25°C for CO. Furthermore, k_s corresponds to the mass transfer coefficient determined from the work of Ingersoll and Inman[31] and Liebl[29] with CO. Unfortunately, data determined with CO cannot be extended to other species, such as CH_4, as is possible with the ocean absorption. This is readily appreciated since the soil's chemical and biological action would be different for each species.

Leakage to the Troposphere

Leakage to or from the troposphere creates what may be classified as artificial sources or sinks. If a complete atmospheric global dispersion model were the object, these effects would not be realized as sources and sinks. However, model complexity precludes such considerations in the initial simulation.

As a first approximation, the tropopause can be considered as a zero-flux boundary. This would be expressed as

$$-\varepsilon_r \left. \frac{\partial c}{\partial r} \right|_{r=\text{Tropopause}} = F_T \qquad (35),$$

where F_T is zero for the zero flux boundary condition. However, most investigations indicate that F_T, although small, is not zero. Specifically, the analyses of Seiler and Warneck[43] and Machta[44] indicate that for CO, $F_T \sim 5 \times 10^{-11}$ gCO/m^2 sec. With this value of F_T the concentration gradient is quite small and changes in the CO concentration in the upper kilometer or so of the troposphere are less than 0.1%, even for modest values of the eddy diffusivity. Thus, a zero flux condition is a valid first approximation.

NUMERICAL MODEL

In the previous section, the physico-chemical model was described. In this section, the numerical treatment is discussed.

Convective Difference Schemes

One of the primary objectives of numerical schemes for convective problems is to preserve conservation of mass. Some procedures, therefore, employ a flux approach to numerically simulate the problem rather than directly finite-differencing the partial differential equation. These methods have been found very useful in numerical solution of the Navier-Stokes equations and have received significant attention[45-56], especially with regard to turbulent flow calculations and atmospheric fluid motion problems. One of the advantages to solving Equation (18), as compared to the Navier-Stokes equations, is that it has linear convective terms whereas the latter contains nonlinear convective terms. However, the generation terms in Equation (18) do introduce

non-linearities in the proposed studies.

Consider the difference element illustrated in Figure 2. By applying the conservation of mass for any particular species the following equation can be written.

$$\left(\frac{c_{i,j,k}^{n+1} - c_{i,j,k}^{n}}{\Delta t}\right) 8r_k^2 \cos\theta_j \, \Delta\phi \, \Delta\theta \, \Delta r = (F_{i-1,j,k}^{\phi} + J_{i-1,j,k}^{\phi}$$

$$-F_{i+1,j,k}^{\phi} - J_{i+1,j,k}^{\phi}) \, 4r_k \Delta\theta \, \Delta r + (\cos\theta_{j-1} F_{i,j-1,k}^{\theta} + \cos\theta_{j-1} J_{i,j-1,k}^{\theta}$$

$$- \cos\theta_{j+1} F_{i,j+1,k}^{\theta} - \cos\theta_{j+1} J_{i,j+1,k}^{\theta}) 4r_k \, \Delta\phi \, \Delta r + (r_{k-1}^2 F_{i,j,k-1}^{r} + r_{k-1}^2 J_{i,j,k-1}^{r}$$

$$- r_{k+1}^2 F_{i,j,k+1}^{r} - r_{k+1}^2 J_{i,j,k+1}^{r}) 4 \cos\theta_j \, \Delta\phi \, \Delta\theta + R_{i,j,k}^{v} \, 8r_k^2 \cos\theta_j \Delta\phi\Delta\theta\Delta r \quad (36)$$

In Equation (36), i, j, and k refer to the grid point in the ϕ, θ, and r directions, respectively, and n refers to the time level. It should be noted that Equation (36) has been applied over two grid intervals in each direction. $F_{i,j,k}^{\phi}$, $F_{i,j,k}^{\theta}$, and $F_{i,j,k}^{r}$ are the convective fluxes in the superscripted directions and can be related to the velocities in these directions. Following Roberts and Weiss[46] these can be expressed as

$$F_{i,j,k}^{\phi} = \frac{1}{4r_k\Delta\theta\Delta r\Delta t} \int_{t^n}^{t^{n+1}} \int_{\theta_{j-1}}^{\theta_{j+1}} \int_{r_{k-1}}^{r_{k+1}} c(\phi_i,\theta,r,t)u(\phi_i,\theta,r)r \, dr \, d\theta \, dt \quad (37),$$
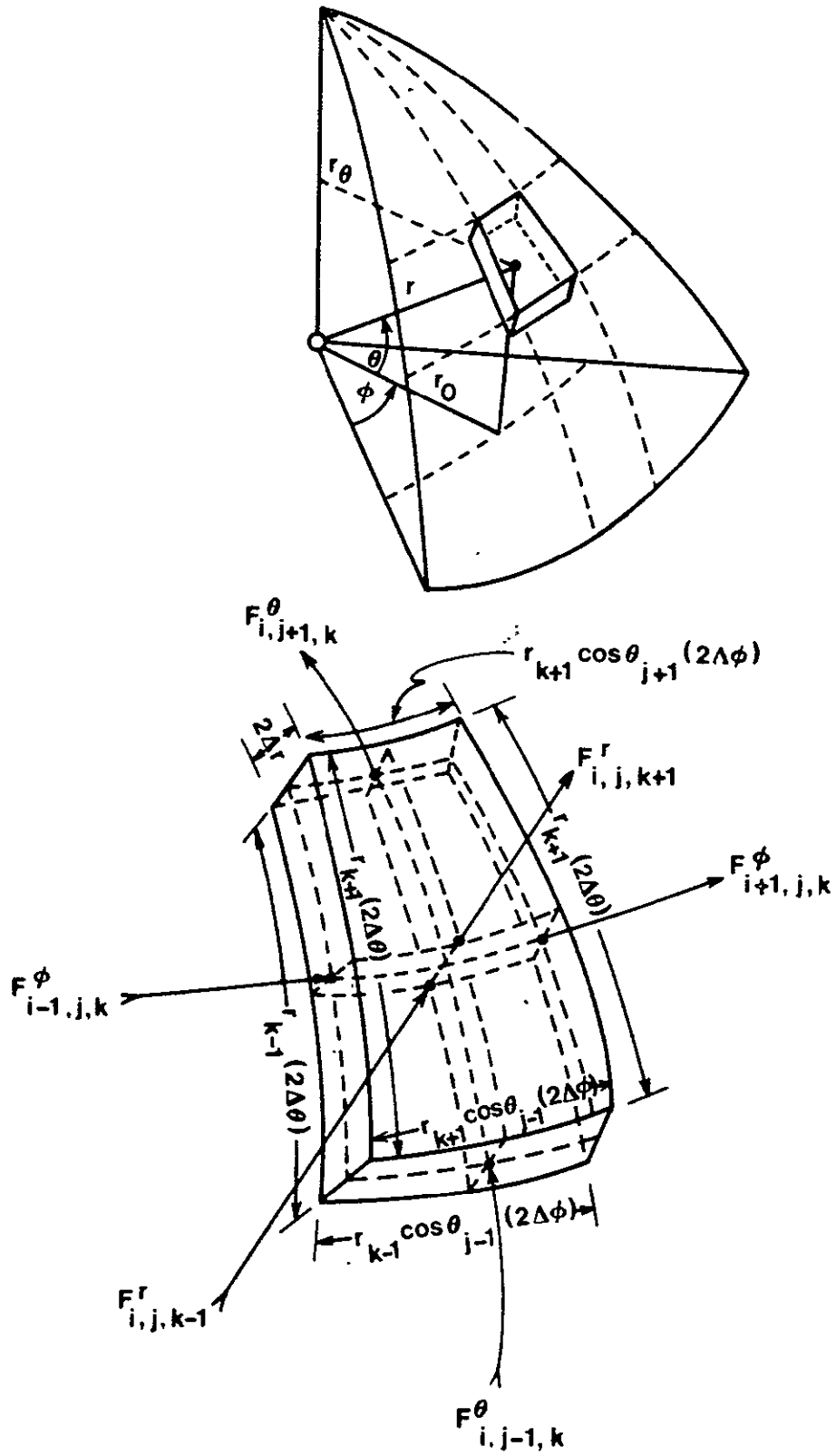
Figure 2

Finite Element for Applying the Conservation of Mass

$$F^\theta_{i,j,k} = \frac{1}{4r_k\cos\theta_j\Delta\phi\Delta r\Delta t} \int_{t^n}^{t^{n+1}} \int_{\phi_{i-1}}^{\phi_{i+1}} \int_{r_{k-1}}^{r_{k+1}} c(\phi,\theta_j,r,t)v(\phi,\theta_j,r)\cos\theta r\, dr\, d\phi\, dt \tag{38},$$

and

$$F^r_{i,j,k} = \frac{1}{4r_k^2\cos\theta_j\Delta\phi\Delta\theta\Delta t} \int_{t^n}^{t^{n+1}} \int_{\phi_{i-1}}^{\phi_{i+1}} \int_{\theta_{j-1}}^{\theta_{j+1}} c(\phi,\theta,r_k,t)w(\phi,\theta,r_k)r^2\cos\theta\, d\theta\, d\phi\, dt \tag{39}.$$

Development of Equations (37) thru (39) in difference form is the central point in establishing the numerical accuracy level, and for the current work it is fourth order in the convective terms. $J^r_{i,j,k}$, $J^\phi_{i,j,k}$, and $J^\theta_{i,j,k}$ represent the diffusive fluxes in each of the superscripted directions. These are expressible in gradient form.

Anticipating the development of the convective fluxes, the diffusive terms will be evaluated using the intermediate time level, n + 1/2, as well as the time levels n and n+1. After differencing the diffusive flux terms, Equation (36) can be rewritten as

$$x^{n+1}_{i,j,k} C_{i,j,k} = x^n_{i,j,k} C_{i,j,k} + (F^\phi_{i-1,j,k} - F^\phi_{i+1,j,k}) \frac{\Delta t}{2r_k \cos\theta_j \Delta\phi}$$

$$+ (\cos\theta_{j-1} F^\theta_{i,j-1,k} - \cos\theta_{j+1} F^\theta_{i,j+1,k}) \frac{\Delta t}{2r_k \cos\theta_j \Delta\theta}$$

$$+ (r^2_{k-1} F^r_{i,j,k-1} - r^2_{k+1} F^r_{i,j,k+1}) \frac{\Delta t}{2r_k^2 \Delta r}$$

$$+ (x^{n+1/2}_{i,j,k+1} + x^{n+1/2}_{i,j,k-1} - x^{n+1}_{i,j,k} - x^n_{i,j,k}) \frac{\varepsilon_r C_{i,j,k}\Delta t}{\Delta r^2}$$

$$+ (x_{i,j,k+1}^{n+1/2} - x_{i,j,k-1}^{n+1/2}) \frac{\varepsilon_r C_{i,j,k} \Delta t}{r_k \Delta r}$$

$$+ (C_{i,j,k+1} - C_{i,j,k-1})(x_{i,j,k+1}^{n+1/2} - x_{i,j,k-1}^{n+1/2}) \frac{\varepsilon_r \Delta t}{4\Delta r^2}$$

$$+ (x_{i,j+1,k}^{n+1/2} + x_{i,j-1,k}^{n+1/2} - x_{i,j,k}^{n+1} - x_{i,j,k}^{n}) \frac{\varepsilon_\theta C_{i,j,k} \Delta t}{r_k^2 \Delta \theta^2}$$

$$+ (C_{i,j+1,k} - C_{i,j-1,k})(x_{i,j+1,k}^{n+1/2} - x_{i,j-1,k}^{n+1/2}) \frac{\varepsilon_\theta \Delta t}{4r_k^2 \Delta \theta^2}$$

$$- (x_{i,j+1,k}^{n+1/2} - x_{i,j-1,k}^{n+1/2}) \frac{\varepsilon_\theta C_{i,j,k} \tan\theta_j \Delta t}{2r_k^2 \Delta \theta} + (x_{i+1,j,k}^{n+1/2} + x_{i-1,j,k}^{n+1/2}$$

$$- x_{i,j,k}^{n+1} - x_{i,j,k}^{n}) \frac{\varepsilon_\phi C_{i,j,k} \Delta t}{r_k^2 \cos^2\theta_j \Delta\phi^2} + (C_{i+1,j,k}$$

$$- C_{i-1,j,k})(x_{i+1,j,k}^{n+1/2} - x_{i-1,j,k}^{n+1/2}) \frac{\varepsilon_\phi \Delta t}{4r_k^2 \cos^2\theta_j \Delta\phi^2} + R_{i,j,k}^v \Delta t \qquad (40).$$

In Equation (40), $x_{i,j,k}^{n}$ represents the mole fraction of the species being considered, and $C_{i,j,k}$ represents the molar density of the air determined from the prevailing temperature and pressure.

The formulation of the diffusive flux difference terms uses a central difference scheme, which is essentially second order accurate. Roberts and Weiss[46] state that this method is unconditionally stable and sufficiently accurate as long as ε is small. Certainly in the horizontal motions this is true; however, subgrid scale motions usually

will dominate the vertical fluxes, and ε_r may not be considered small.
Thus, it could be qualitatively argued that the procedure is essentially
fourth order accurate in θ and ϕ but only second order accurate in r,
as well as time. However, this drawback is easily overcome since the
mesh size in the radial or vertical direction will be considerably smaller
than the mesh length in the horizontal. Therefore, it appears that the
accuracy of the scheme is still limited by the order of accuracy of the
horizontal motions.

The generation term in Equation (40) is a volume average over the
region $i\pm1$, $j\pm1$, $k\pm1$, and over time Δt. Thus, it can be expressed as

$$R^v_{i,j,k} = \frac{1}{8r_k^2\cos\theta_j\,\Delta\phi\Delta\theta\Delta r\Delta t} \int_{t^n}^{t^{n+1}} \int_{\phi_{i-1}}^{\phi_{i+1}} \int_{\theta_{j-1}}^{\theta_{j+1}} \int_{r_{k-1}}^{r_{k+1}} R(\phi,\theta,r,t)r^2\cos\theta\,dr\,d\theta\,d\phi\,dt \quad (41).$$

It should be noted at this point that the generation terms will be
determined from concentrations already calculated. An alternative
scheme would be to calculate the concentration of one species at the
new time level using the intermediate time level. Then this updated con-
centration could be employed in the generation term for the next species.
This might improve the computational stability characteristics but would
have to be established by numerical experiments. These types of schemes
are necessary in order to decouple the three diffusion equations for each
of the three species. Otherwise, the three equations would have to be
solved simultaneously, which, due to their nature, would either require
linearization or some iterative scheme. It is felt that these procedures
are not justified. The individual generation terms can then be found
from Equation (22) thru Equation (24).

It is now appropriate to further consider the flux and generation terms, thus far only expressed in integral form. By expanding the product of concentration and velocity in a Taylor series in space and time, any desired accuracy can be achieved. For each of the flux terms, the following results can be obtained.

$$F^{\phi}_{i,j,k} = (cu)^{\phi}_{i,j,k} + 1/3 \; (\frac{\partial c}{\partial \theta} \frac{\partial u}{\partial \theta})^{n+1/2}_{i,j,k} \Delta\theta^2 + 1/3 \; (\frac{\partial c}{\partial r} \frac{\partial u}{\partial r})^{n+1/2}_{i,j,k} \Delta r^2$$

$$+ \; 0(\Delta t^2, \; \Delta\theta^p r^{4-p}) \tag{42}$$

$$F^{\theta}_{i,j,k} = (cv)^{\theta}_{i,j,k} + 1/3 \; (\frac{\partial c}{\partial \phi} \frac{\partial v}{\partial \phi})^{n+1/2}_{i,j,k} \Delta\phi^2$$

$$+ \; 1/3 \; (\frac{\partial c}{\partial r} \frac{\partial v}{\partial r})^{n+1/2}_{i,j,k} \Delta r^2 + 0(\Delta t^2, \; \Delta\phi^p r^{4-p}) \tag{43}$$

$$F^{r}_{i,j,k} = (cw)^{r}_{i,j,k} \frac{\Delta\theta}{\sin \Delta\theta} + 1/3 \; (\frac{\partial c}{\partial \phi} \frac{\partial w}{\partial \phi})^{n+1/2}_{i,j,k} \frac{\sin \Delta\theta}{\Delta\theta} \Delta\phi^2$$

$$+ \; 2 \; (\frac{\partial c}{\partial \theta} \frac{\partial w}{\partial \theta})^{n+1/2}_{i,j,k} (\cos \Delta\theta - \frac{2-\Delta\theta^2}{2} \frac{\sin \Delta\theta}{\Delta\theta})$$

$$+ \; 0(\Delta t^2, \; \Delta\theta^p \phi^{4-p}) \tag{44}$$

We will be content with fourth-roder accuracy in the space variable and second order in time as indicated by terms $0(\Delta t^2, \Delta-)$. It should be noted that in order to' assure second order accuracy in time, the direction of integration must reverse with each time step. Furthermore, for $\theta_j > 45°$

the accuracy in the θ-space variable is decreased. However, at θ_j as large as 85° the accuracy is apparently still third-order.

Roberts and Weiss[46] suggest expressing the zeroth-order terms in a manner as illustrated below.

$$(cu)_{i,j,k}^{\phi} = 1/6 \ [u_{i,j,k}(8c_{i,j,k}^{n+1/2} - c_{i-1,j,k}^{n+1} - c_{i+1,j,k}^{n})] \qquad (45)$$

Equation (45) alternates with the following form for the reverse direction integration.

$$(cu)_{i,j,k}^{\phi} = 1/6 \ [u_{i,j,k}(8c_{i,j,k}^{n+1/2} - c_{i-1,j,k}^{n} - c_{i+1,j,k}^{n+1})] \qquad (46)$$

The derivatives in Equations (42), (43), and (44) are differenced using a central difference scheme.

The generation term described by Equation (41) can be handled in a manner slightly different than the flux terms. The result is

$$R_{i,j,k}^{v} = [R_{i,j,k}^{n+1/2} + 1/6 \ (\frac{\partial^2 R}{\partial \phi^2})_{i,j,k}^{n+1/2} \Delta\phi^2 + 1/6 \ (\frac{\partial^2 R}{\partial r^2})_{i,j,k}^{n+1/2} \Delta r^2] \ \frac{\sin \Delta\theta}{\Delta\theta}$$

$$+ (\frac{\partial R}{\partial \theta})_{i,j,k}^{n+1/2} \tan \theta_j \ (\cos \Delta\theta - \frac{\sin \Delta\theta}{\Delta\theta})$$

$$+ (\frac{\partial^2 R}{\partial \theta^2})_{i,j,k}^{n+1/2} \ (\cos \Delta\theta - \frac{2 - \Delta\theta^2}{2} \frac{\sin \Delta\theta}{\Delta\theta}) \qquad (47).$$

Again, the order of accuracy is reduced slightly for θ_j larger than 45°.

Due to the complex algegraic form of the generation terms, $R_{i,j,k}^{n+1/2}$ is just calculated from data at the intermediate time level.

The above discussion briefly describes the numerical procedure. Additional detail can be found in the appendix at the end of this chapter. The numerical integration is initiated by considering grid elements surrounding either pole. Since the area at the poles for imput of mass is zero, the concentrations at the latitudes 10° from either pole do not directly depend on the concentrations at the poles.

Representation of Sub-Grid Scale Motions

Since the numerical approximation of the transport of mass attempts to represent a continuum by a discrete set of points, one must consider the effect of the small scale motions on the large scale convection. In any finite numerical model of turbulent flow processes, it is unrealistic to assume that motions of all scales can be simulated. Rather, one must be content to explicity evaluate the large scale convection and to parameterize the small scale mixing processes.

This can be more readily appreciated by considering the appropriately averaged species equation of continuity. Rather than time averaging the equations in the Reynolds sense as is customarily done, it is more useful to volume average over a given grid. Time averaging, in essence, represents all turbulent processes by the time averaged product of the deviation variables (e.g., $\overline{u'v'}$, $\overline{u'c'}$, etc). However, in numerical treatment of the equations of change some of the motions that would be considered turbulent in the Reynolds sense may be

calculated explicity in time if the grid size is sufficiently small. Therefore, it is expected that the eddy diffusivity one uses to approximate the sub-grid scale motions depends on the grid size.

More specifically, let the grid-scale averaging operator (represented by an overbar) be defined as follows:

$$\bar{u} = \frac{1}{r^2 \cos\theta \Delta\phi\Delta\theta\Delta\,r} \int_{\Delta r} \int_{\Delta\theta} \int_{\Delta\phi} u(\phi,\theta,r,t) r^2 \cos\theta \; d\phi \, d\theta \, dr \qquad (48)$$

or

$$\bar{c} = \frac{1}{r^2 \cos\,\theta\Delta\phi\Delta\theta\Delta\,r} \int_{\Delta r} \int_{\Delta\theta} \int_{\Delta\phi} c(\phi,\theta,r,t) \; r^2 \cos\theta \; d\phi \; d\theta \; dr \qquad (49)$$

The grid-averaged variable ($\bar{u}$ or $\bar{c}$) is now a continuous function of space and time. If one lets u' and c' represent deviations from local grid-volume means, it is easy to recognize that terms analogous to the conventionally time averaged ones are obtained. However, there is the important difference between the two terms as to what portion of the turbulent processes do the two represent.

There has been considerable attention, relative to solving the Navier-Stokes Equation, devoted to the concept of using a grid size dependent viscosity (sometimes referred to as an aritficial viscosity) to describe the micro-scale phenomena[57-60]. Deardorff[51], Crowley[61], Manabe, Smagorinsky, Holloway, and Stone[62] and others have employed such viscosities for fluid dynamics calculations. The

eddy viscosity can be based on either a local kinetic energy dissipation

rate or an average kinetic energy dissipation rate. In the former case

the resulting eddy viscosity is non-linear while in the latter case

there is a single value for the entire space.

Smagorinsky, Manabe, and Holloway[57], Leith[59], and Monin and

Zilitinkevich[60] have used the well-known dimensional analysis

approach of Kolmogorov for three-dimensional homogeneous turbulence

to relate the eddy viscosity to the local rate of strain. Let α_1 be

a dimensionless constant and let Δ_3 be the cube root of the product

of the mesh spacing (for rectangular cartesian coordinates, $\Delta_3 =$

$(\Delta_{x_1} \cdot \Delta_{x_2} \cdot \Delta_{x_3})^{1/3}$), then

$$\varepsilon = (\alpha_1 \Delta_3)^2 \left[\frac{\partial \bar{u}_i}{\partial x_j} \left(\frac{\partial \bar{u}_i}{\partial x_j} + \frac{\partial \bar{u}_j}{\partial x_i} \right) \right]^{1/2} \tag{50}.$$

In Equation (50) the Einstein convention for tensor notation is used for

simplicity. Deardorff's[51] calculation for turbulent channel flow

indicated that $\alpha_1 = 0.10$ was optimum.

Leith, however, argues that Equation (50) is of dubious validity

in global numerical models since the horizontal grid is much larger

than the vertical grid and thus is inconsistent with three dimensional

isotropy. Instead, he treats the grid scale as being two dimensional

and uses dimensional arguments based on the cascade of vorticity (ω)

in two dimensions to arrive at

$$\varepsilon = \alpha \, {}_2^{3/2} \, |\nabla \omega| \Delta_2^3 \qquad . \qquad (51)$$

where $\Delta_2 = (\Delta_{x_1} \cdot \Delta_{x_2})^{1/2}$. Crowley's[61] experiments on wind driven ocean circulations suggest that $\alpha_2 = 0.05$.

It is clear that Equations (50) and (51) lead to non-linear eddy viscosities which are local. Monin[60] has suggested that a linear viscosity can be estimated as

$$\varepsilon \sim \varepsilon \, {}_0^{1/3} \, \Delta^{4/3} \qquad (52),$$

where ε_0 is the kinetic energy dissipation averaged for the whole calculation space. For the entire atmosphere, $\varepsilon_0 \sim 5$ erg/g sec. To intuitively extend this concept one might consider ε to be axis dependent and write

$$\varepsilon_{x_i} \sim \varepsilon_0^{1/3} \, \Delta_{x_i}^{4/3} \qquad (53).$$

While the simplicity of the linear viscosity is retained for computational purposes, Equation (53) does permit different scaling of the micro-scale phenomena in the three directions. The results of Deardorff[51] show the constant of proportionality in Equation (53) to be $(0.094)^{4/3}$.

The discussion of the representation of sub-grid scale motions has thus far been restricted to momentum exchange. However, since our interests are in mass exchange the extension to eddy diffusivity must be made. The obvious appraoch is to assume that the turbulent Schmidt

number (the ratio of the eddy viscosity to eddy diffusivity) is one.
In addition, further detailing of approximations for the eddy diffusivity
is hardly jusitifed at the present until more and better atmospheric
turbulent exchange data are obtained. Based on these discussions, the
following values for the eddy diffusivities would be consistent with
grid spacings of 10° x 10° x 2.5 km: $\varepsilon_\phi = \varepsilon_\theta = 10^5 m^2/sec$ and $\varepsilon_r = 10^2$
m^2/sec. These values are in agreement with the suggestions of Lilly[47]
and Deardorff[51] and with the linear viscosity used by Crowley[61]
for ocean circulation calculations employing a smaller grid size.

SUMMARY

In this chapter, we have discussed the development of a global
transport/chemistry circulation model that accounts for natural and
anthropogenic sources of pollutants. Specifically the geochemically
important methane – carbon monoxide system is described in which the
oxidation of methane leads to the formation of carbon monoxide. The
pseudo-steady state approximation is exploited for the reactive inter-
mediate species so that the number of species continuity equations
that must be solved is reduced to a minimum. By so doing three dim-
ensionality of the solution can still be retained.

The incorporation of the physico-chemical behavior of the species
into the model is discussed in sufficient generality that the proce-
dures described could be readily extended to other important systems.
Such efforts should be encouraged. In the subsequent chapter, the
results to date of computer simulations of the methane-carbon monoxide
system are described.

APPENDIX A

DETAILS OF NUMERICAL SOLUTION

In order to conveniently express Equation (40) we will define modified flux terms for $F^{\phi}_{i+1,j,k}$, $F^{\theta}_{i,j+1,k}$, and $F^{r}_{i,j,k+1}$. These are

$$\hat{F}^{\phi}_{i+1,j,k} = \frac{1}{6} u_{i+1,j,k} (8c^{n+1/2}_{i+1,j,k} - c^{n}_{i+2,j,k})$$

$$+ \frac{1}{3} \left(\frac{\partial c}{\partial \theta} \frac{\partial u}{\partial \theta}\right)^{n+1/2}_{i+1,j,k} \Delta\theta^2 + \frac{1}{3} \left(\frac{\partial c}{\partial r} \frac{\partial u}{\partial r}\right)^{n+1/2}_{i+1,j,k} \Delta r^2 \qquad (A-1),$$

$$\hat{F}^{\theta}_{i,j+1,k} = \frac{1}{6} v_{i,j+1,k} (8c^{n+1/2}_{i,j+1,k} - c^{n}_{i,j+2,k})$$

$$+ \frac{1}{3} \left(\frac{\partial c}{\partial \phi} \frac{\partial v}{\partial \phi}\right)^{n+1/2}_{i,j+1,k} \Delta\phi^2 + \frac{1}{3} \left(\frac{\partial c}{\partial r} \frac{\partial v}{\partial r}\right)^{n+1/2}_{i,j+1,k} \Delta r^2 \qquad (A-2),$$

$$\hat{F}^{r}_{i,j,k+1} = \frac{1}{6} w_{i,j,k+1} (8c^{n+1/2}_{i,j,k+1} - c^{n}_{i,j,k+2}) \frac{\Delta\theta}{\sin\Delta\theta} + \frac{1}{3} \left(\frac{\partial c}{\partial \phi} \frac{\partial w}{\partial \phi}\right)^{n+1/2}_{i,j,k+1} \frac{\sin\Delta\theta}{\Delta\theta} \Delta\phi^2$$

$$+ 2 \left(\frac{\partial c}{\partial \theta} \frac{\partial w}{\partial \theta}\right)^{n+1/2}_{i,j,k+1} (\cos \Delta\theta - \frac{2 - \Delta\theta^2}{2} \frac{\sin \Delta\theta}{\Delta\theta}) \qquad (A-3).$$

Let x, y, and z represent the mole fraction of methane, formaldehyde, and carbon monoxide, respectively. The concentration of each species at the updated time can then be found by solving the following system of equations.

$$C_{i,j,k} (1 - \frac{u_{i+1,j,k}\Delta t}{12r_k \cos\theta_j \Delta\theta} - \frac{\cos\theta_{j+1} v_{i,j+1,k}\Delta t}{12r_k \cos\theta_j \Delta\theta} - \frac{r^2_{k+1} w_{i,j,k+1}\Delta\theta\Delta t}{12r^2_k \sin \Delta\theta \Delta r}$$

$$+ \frac{\varepsilon_\phi \Delta t}{r^2_k \cos^2\theta_j \Delta\phi^2} + \frac{\varepsilon_\theta \Delta t}{r^2_k \Delta\theta^2} + \frac{\varepsilon_r \Delta t}{\Delta r^2})x^{n+1}_{i,j,k}$$

$$+ \frac{u_{i-1,j,k} C_{i-2,j,k} \Delta t}{12 \, r_k \cos \theta_j \, \Delta \phi} x^{n+1}_{i-2,j,k} + \frac{r^2_{k-1} w_{i,j,k-1} C_{i,j,k-2} \Delta t}{12 \, r^2_k \, \Delta r} x^{n+1}_{i,j,k-2} =$$

$$C_{i,j,k} x^n_{i,j,k} + (\hat{F}^{\phi,x}_{i-1,j,k} - \hat{F}^{\phi,x}_{i+1,j,k}) \frac{\Delta t}{2 r_k \cos \theta_j \, \Delta \phi}$$

$$- \frac{\cos\theta_{j-1} v_{i,j-1,k} C_{i,j-2,k} \Delta t}{12 \, r_k \cos \theta_j \, \Delta \theta} x^{n+1}_{i,j-2,k} + (\cos\theta_{j-1} \hat{F}^{\theta,x}_{i,j-1,k}$$

$$- \cos\theta_{j+1} \hat{F}^{\theta,x}_{i,j+1,k}) \frac{\Delta t}{2 \, r_k \cos \theta_j \, \Delta \theta}$$

$$+ (r^2_{k-1} \hat{F}^{r,x}_{i,j,k-1} - r^2_{k+1} \hat{F}^{r,x}_{i,j,k+1}) \frac{\Delta t}{2 r^2_k \Delta r} + (x^{n+1/2}_{i+1,j,k} + x^{n+1/2}_{i-1,j,k}$$

$$- x^n_{i,j,k}) \frac{\epsilon_\phi C_{i,j,k} \Delta t}{r^2_k \cos^2\theta_j \Delta\phi^2} + (C_{i+1,j,k} - C_{i-1,j,k})(x^{n+1/2}_{i+1,j,k}$$

$$- x^{n+1/2}_{i-1,j,k}) \frac{\epsilon_\phi \Delta t}{4 r^2_k \cos^2\theta_j \Delta\phi^2} + (x^{n+1/2}_{i,j+1,k} + x^{n+1/2}_{i,j-1,k}$$

$$- x^n_{i,j,k}) \frac{\epsilon_\theta C_{i,j,k} \Delta t}{r^2_k \Delta\theta^2} + (C_{i,j+1,k} - C_{i,j-1,k})(x^{n+1/2}_{i,j+1,k}$$

$$- x^{n+1/2}_{i,j-1,k}) \frac{\epsilon_\theta \Delta t}{4 r^2_k \Delta\theta^2} - (x^{n+1/2}_{i,j+1,k} - x^{n+1/2}_{i,j-1,k}) \frac{\epsilon_\theta C_{i,j,k} \tan \theta_j \, \Delta t}{2 r^2_k \, \Delta\theta}$$

$$+ (x^{n+1/2}_{i,j,k+1} + x^{n+1/2}_{i,j,k-1} - x^n_{i,j,k}) \frac{\epsilon_r C_{i,j,k} \Delta t}{\Delta r^2} + (x^{n+1/2}_{i,j,k+1}$$

$$- x^{n+1/2}_{i,j,k-1}) \frac{\epsilon_r C_{i,j,k} \Delta t}{r_k \Delta r} + (C_{i,j,k+1} - C_{i,j,k-1})(x^{n+1/2}_{i,j,k+1}$$

$$- x^{n+1/2}_{i,j,k-1}) \frac{\epsilon_r \Delta t}{4\Delta r^2} + R^{v,x}_{i,j,k} \Delta t \tag{A-4}$$

Thus $\hat{F}^{\phi,x}_{i-1,j,k}$, $\hat{F}^{\phi,x}_{i+1,j,k}$, $\hat{F}^{\theta,x}_{i,j-1,k}$, $\hat{F}^{\theta,x}_{i,j+1,k}$, $\hat{F}^{r,x}_{i,j,k-1}$, $\hat{F}^{r,x}_{i,j,k+1}$, and

$R^{v,x}_{i,j,k}$ are computed and then Equation (A-4) is solved. Similar relationships can be written for the formaldehyde and carbon monoxide concentrations.

Grid boxes that occur on a boundary of the region being considered can be treated using the integral flux method in a similar manner. As an example, consider the surface boundary where there is a grid box of dimension $2\Delta\phi$, $2\Delta\theta$ and Δr. By using the integral formulation, we can express the increment in the concentration of a particular species as

$$x^{n+1}_{i,j,1}C_{i,j,1} = x^{n}_{i,j,1}C_{i,j,1} + (F^{\phi}_{i-1,j,1} - F^{\phi}_{i+1,j,1}) \frac{\Delta t}{2r_1 \cos\theta_j \Delta\phi}$$

$$+ (\cos\theta_{j-1}F^{\theta}_{i,j-1,1} - \cos\theta_{j+1}F^{\theta}_{i,j+1,1}) \frac{\Delta t}{2r_1 \cos\theta_j \Delta\theta} + (r_2^2 F^{r}_{i,j,1}$$

$$- r_2^2 F^{r}_{i,j,2} - r_2^2 J^{r}_{i,j,2}) \frac{\Delta t}{r_1^2 \Delta r} + (x^{n+1/2}_{i,j+1,1} + x^{n+1/2}_{i,j-1,1} - x^{n+1}_{i,j,1}$$

$$- x^{n}_{i,j,1}) \frac{\varepsilon_{\theta}C_{i,j,1}\Delta t}{r_1^2 \Delta\theta^2} + (C_{i,j+1,1} - C_{i,j-1,1})(x^{n+1/2}_{i,j+1,1}$$

$$- x^{n+1/2}_{i,j-1,1}) \frac{\varepsilon_{\theta} \Delta t}{4r_1^2 \Delta\theta^2} - (x^{n+1/2}_{i,j+1,1} - x^{n+1/2}_{i,j-1,1}) \frac{\varepsilon_{\theta}C_{i,j,1}\tan\theta_j \Delta t}{2r_1^2 \Delta\theta}$$

$$+ (x^{n+1/2}_{i+1,j,1} + x^{n+1/2}_{i-1,j,1} - x^{n+1}_{i,j,1} - x^{n}_{i,j,1}) \frac{\varepsilon_{\phi}C_{i,j,1}\Delta t}{r_1^2 \cos^2\theta_j \Delta\phi^2}$$

$$+ (C_{i+1,j,1} - C_{i-1,j,1})(x^{n+1/2}_{i+1,j,1} - x^{n+1/2}_{i-1,j,1}) \frac{\varepsilon_{\phi}\Delta t}{4r_1^2 \cos^2\theta_j \Delta\phi^2}$$

$$+ R^{v}_{i,j,1}\Delta t \qquad\qquad (A-5).$$

It should be noted that values of $x_{i,j,1}$ should be regarded as averages over boxes centered on ϕ_i, θ_j, $r_{3/2}$. $J_{i,j,2}^r$ can be expressed in a central finite difference form, which employs stored values, as follows:

$$J_{i,j,2}^r = -\frac{\varepsilon_r}{4\Delta r}[2\,c_{i,j,3}x_{i,j,3}^{n+1/2} - c_{i,j,1}(x_{i,j,1}^n + x_{i,j,1}^{n+1})] \qquad (A-6)$$

Furthermore, the ground level flux term must account for both a constant area source (S_G) as well as an ocean or soil type source. Thus,

$$\mathscr{F}_{i,j,1}^r = \frac{1}{4r_1^2\cos\theta_j\,\Delta\phi\Delta\theta\Delta t}\int_{t^n}^{t^{n+1}}\int_{\phi_{i-1}}^{\phi_{i+1}}\int_{\theta_{j-1}}^{\theta_{j+1}}[K_G(c_G^* - c) + S_G](\phi,\theta,r_1,t)\,r_1^2\cos\theta\,d\theta\,d\phi\,dt$$

$$(A-7),$$

which to a fourth-order approximation can be written as

$$\mathscr{F}_{i,j,1}^r = \frac{1}{2}\{[K_G(c_G^* - c) + S_G]_{i,j,1}^n + [K_G(c_G^* - c) + S_G]_{i,j,1}^{n+1}\}\,\frac{\sin\Delta\theta}{\Delta\theta} +$$

$$\frac{1}{6}\left[\frac{\partial^2[K_G(c_G^* - c) + S_G]}{\partial\phi^2}\right]_{i,j,1}^{n+1/2}\frac{\sin\Delta\theta}{\Delta\theta}\Delta\phi^2 + \left[\frac{\partial[K_G(c_G^* - c) + S_G]}{\partial\theta}\right]_{i,j,1}^{n+1/2}\tan\theta_j\left(\cos\Delta\theta - \frac{\sin\Delta\theta}{\Delta\theta}\right)$$

$$+ \left[\frac{\partial^2[K_G(c_G^* - c) + S_G]}{\partial\theta^2}\right]_{i,j,1}^{n+1/2}\left(\cos\Delta\theta - \frac{2-\Delta\theta^2}{2}\frac{\sin\Delta\theta}{\Delta\theta}\right) \qquad (A-8).$$

The convective fluxes can be conveniently expressed as

$$F^{\phi}_{i,j,1} = \frac{1}{2} \left[(cu)^{n+1/2}_{i,j,1} + (cu)^{n+1/2}_{i,j,2} \right] + \frac{1}{12} \left\{ \left[\frac{\partial^2 (cu)}{\partial \theta^2} \right]^{n+1/2}_{i,j,1} \Delta\theta^2 \right.$$

$$+ \left[\frac{\partial^2 (cu)}{\partial \theta^2} \right]^{n+1/2}_{i,j,2} \Delta\theta^2 + \frac{3}{4} \left[\frac{\partial^2 (cu)}{\partial r^2} \right]^{n+1/2}_{i,j,2} \Delta r^2 - \frac{1}{4} \left[\frac{\partial^2 (cu)}{\partial r^2} \right]^{n+1/2}_{i,j,3} \Delta r^2 \right\}$$

$$(A-9),$$

and

$$F^{\theta}_{i,j,1} = \frac{1}{2} \left[(cv)^{n+1/2}_{i,j,1} + (cv)^{n+1/2}_{i,j,2} \right] + \frac{1}{12} \left\{ \left[\frac{\partial^2 (cv)}{\partial \phi^2} \right]^{n+1/2}_{i,j,1} \Delta\phi^2 \right.$$

$$+ \left[\frac{\partial^2 (cv)}{\partial \phi^2} \right]^{n+1/2}_{i,j,2} \Delta\phi^2 + \frac{3}{4} \left[\frac{\partial^2 (cv)}{\partial r^2} \right]^{n+1/2}_{i,j,2} \Delta r^2 - \frac{1}{4} \left[\frac{\partial^2 (cv)}{\partial r^2} \right]^{n+1/2}_{i,j,3} \Delta r^2 \right\}$$

$$(A-10).$$

The vertical convective flux $F^{r}_{i,j,2}$ can be obtained by Equation (44), and the generation term will be written as

$$R^{v}_{i,j,1} = \frac{1}{2} \left[R^{n+1/2}_{i,j,1} + R^{n+1/2}_{i,j,3} + \frac{1}{6} \left(\frac{\partial^2 R}{\partial \phi^2} \right)^{n+1/2}_{i,j,1} \Delta\phi^2 + \frac{1}{6} \left(\frac{\partial^2 R}{\partial \phi^2} \right)^{n+1/2}_{i,j,2} \Delta\phi^2 \right.$$

$$+ \frac{3}{24} \left(\frac{\partial^2 R}{\partial r^2} \right)^{n+1/2}_{i,j,2} \Delta r^2 - \frac{1}{24} \left(\frac{\partial^2 R}{\partial r^2} \right)^{n+1/2}_{i,j,3} \Delta r^2 \right] \frac{\sin \Delta\theta}{\Delta\theta}$$

$$+ \frac{1}{2} \left[\left(\frac{\partial R}{\partial \theta} \right)^{n+1/2}_{i,j,1} + \left(\frac{\partial R}{\partial \theta} \right)^{n+1/2}_{i,j,2} \right] \tan \theta_j \left(\cos \Delta\theta - \frac{\sin \Delta\theta}{\Delta\theta} \right)$$

$$+ \frac{1}{2} \left[\left(\frac{\partial^2 R}{\partial \theta^2} \right)^{n+1/2}_{i,j,1} + \left(\frac{\partial^2 R}{\partial \theta^2} \right)^{n+1/2}_{i,j,2} \right] \left(\cos \Delta\theta - \frac{2 - \Delta\theta^2}{2} \frac{\sin\Delta\theta}{\Delta\theta} \right) \quad \text{(A-11)}.$$

Analogous to Equations (A-1) thru (A-3), define

$$\hat{\mathscr{F}}^r_{i,j,1} = \mathscr{F}^r_{i,j,1} + \frac{1}{2} K_G c^{n+1}_{i,j,1} \frac{\sin \Delta\theta}{\Delta\theta}$$

or

$$\hat{\mathscr{F}}^r_{i,j,1} = \frac{1}{2} \{ [K_G(c^*_G - c) + S_G]^n_{i,j,1} + (K_G c^*_G + S_G)_{i,j,1} \} \frac{\sin \Delta\theta}{\Delta\theta}$$

$$+ \frac{1}{6} \left[\frac{\partial^2 [K_G(c^*_G - c) + S_G]}{\partial \phi^2} \right]^{n+1/2}_{i,j,1} \frac{\sin}{\Delta\theta} \Delta\phi^2 + \left[\frac{\partial [K_G(c^*_G - c) + S_G]}{\partial \theta} \right]^{n+1/2}_{i,j,1} \tan\theta_j \left(\cos \Delta\theta - \frac{\sin\Delta\theta}{\Delta\theta} \right)$$

$$+ \left[\frac{\partial^2 [K_G(c^*_G - c) + S_G]}{\partial \theta^2} \right]^{n+1/2}_{i,j,1} \left(\cos \Delta\theta - \frac{2 - \Delta\theta^2}{2} \frac{\sin\Delta\theta}{\Delta\theta} \right) \quad \text{(A-12)}.$$

With these equations, the concentration at the new time level for a boundary grid can be calculated as follows

$$x^{n+1}_{i,j,1} = \{ x^n_{i,j,1} c_{i,j,1} + (F^{\phi,x}_{i-1,j,1} - F^{\phi,x}_{i+1,j,1}) \frac{\Delta t}{2r_1 \cos\theta_j \Delta\phi} $$

$$+ (\cos \theta_{j-1} F^{\theta,x}_{i,j-1,1} - \cos \theta_{j+1} F^{\theta,x}_{i,j+1,1}) \frac{\Delta t}{2r_1 \cos\theta_j \Delta\theta}$$

$$- \hat{F}^{r,x}_{i,j,2} \frac{r_2^2 \Delta t}{r_1^2 \Delta r} + \hat{\mathscr{F}}^{r,x}_{i,j,1} \frac{\Delta t}{\Delta r}$$

$$+ (2c_{i,j,3} x^{n+1/2}_{i,j,3} - c_{i,j,1} x^n_{i,j,1}) \frac{\varepsilon_r r_2^2 \Delta t}{4r_1^2 \Delta r^2}$$

$$+ (x_{1,j+1,1}^{n+1/2} + x_{1,j-1,1}^{n+1/2} - x_{1,j,1}^{n}) \frac{\varepsilon_\theta C_{1,j,2} \Delta t}{r_1^2 \Delta \theta^2} + (C_{i,j+1,1}$$

$$- C_{1,j-1,1}) (x_{1,j+1,1}^{n+1/2} - x_{1,j-1,1}^{n+1/2}) \frac{\varepsilon_\theta \Delta t}{4 r_1^2 \Delta \theta^2}$$

$$+ (x_{1,j+1,1}^{n+1/2} - x_{1,j-1,1}^{n+1/2}) \frac{\varepsilon_\theta C_{1,j,1} \tan \theta_j \Delta t}{2 r_1^2 \Delta \theta}$$

$$+ (x_{1+1,j,1}^{n+1/2} + x_{1-1,j,1}^{n+1/2} - x_{1,j,1}^{n}) \frac{\varepsilon_\phi C_{1,j,1} \Delta t}{r_1^2 \cos^2 \theta_j \Delta \phi^2}$$

$$+ (C_{1+1,j,1} - C_{1-1,j,1})(x_{1+1,j,1}^{n+1/2} - x_{1-1,j,1}^{n+1/2}) \frac{\varepsilon_\phi \Delta t}{4 r_1^2 \cos^2 \theta_j \Delta \phi^2}$$

$$+ R_{1,j,1}^{v} \Delta t \} / [\ C_{1,j,1} (1 - \frac{1}{6} \frac{w_{1,j,2} r_2^2 \ \Delta \theta \Delta t}{r_1^2 \sin \Delta \theta \Delta r} + \frac{K_{G_{1,j}} \sin \Delta \theta \Delta t}{2 \Delta \theta \Delta r}$$

$$+ \frac{\varepsilon_r r_2^2 \ \Delta t}{4 r_1^2 \ \Delta r^2} + \frac{\varepsilon_\theta \Delta t}{r_1^2 \Delta \theta^2} + \frac{\varepsilon_\phi \ \Delta t}{r_1^2 \cos^2 \theta_j \Delta \phi^2}) \tag{A-13}.$$

Similar developments are made for the tropopause.

CHAPTER 2

RESULTS OF PRELIMINARY SIMULATIONS

The model described in the previous chapter was evaluated in static

and preliminary dynamic transport simulations. Evaluations using the

chemical-kinetic model in a static batch system analysis showed the chem-

ical half lives of CH_4 and CO, their non-chemical source strengths

requisite with reasonable steady state concentrations, and the homo-

geneous chemical source strength of CO by the gas phase oxidation of

CH_4 to be in the proper magnitude. In addition, analysis of the pseudo-

steady state approximation for all of the intermediates, including for-

maldehyde, confirmed its utility and accuracy for simplifying the reaction

scheme when one is not interested in the very short term transient be-

havior of the intermediates.

Preliminary simulations using the transport/chemistry model were

conducted, and the results of this early analysis are described. Chaining

of the isopleths of CH_4 and CO, due to the dominant westerly wind field,

was observed. Longer term simulations are being planned.

INTRODUCTION

In the previous chapter the global transport/chemistry model for

the CH_4 - CO system was described. The physico-chemical considerations

and mathematical development of the numerical model were presented in

substantial detail. In this chapter, we will discuss the results of

44

computer simulations of the model and attempt to compare those results with some of the observations made on the species, especially carbon monoxide.

Static and dynamic transport computer simulations were made. The chemical reaction model was first evaluated assuming a homogeneous reaction system of uniform temperature and pressure without considering any transport of the species. This was a preliminary analysis to judge the validity and evaluate certain aspects of the chemical reaction scheme. Of more significance is the combined transport/chemistry model simulation in which the troposphere's variable properties and the Earth's variable surface are considered. The results of the static and dynamic model computer simulations will be discussed separately in the following sections.

STATIC SIMULATIONS OF CHEMICAL REACTION MODEL

The chemical kinetic model requires as input data the individual reaction rate constants and their temperature dependence, the third body concentrations, and the concentrations of the other chemical entities that are considered time invariant. Rather than using these quantities as adjustable parameters, it was felt that these should be based on the best estimates from the literature. In Table I the reaction rate data and the appropriate references are listed. It should be noted that the temperature dependence is not known for all of the reactions. One should also note that the rate constants k_6, k_7, k_8, k_9, and k_{13}, are not required for the model when the pseudo-steady state

TABLE I

Reaction Rate Constants Employed in Model

Reaction	Rate Constant	Reference
$O_3 + h\nu \rightarrow O(^1D) + O_2$	†$1.05 \times 10^{-5}\ e^{-0.48/\cos\theta}\ sec^{-1}$	2, 63, 64
$O(^1D) + H_2O \rightarrow 2OH$	$3.0 \times 10^{11}\ m^3/kmole\ sec$	64, 65
$O(^1D) + M_3 \rightarrow O + M_3$	$4.8 \times 10^{10}\ m^3/kmole\ sec$	2, 64
$O + O_2 + M_4 \rightarrow O_3 + M_4$	$3.0 \times 10^7\ e^{510/T}\ m^6/kmole^2\ sec$	65, 66
$CH_4 + OH \rightarrow CH_3 + H_2O$	$2.8 \times 10^{10}\ e^{-2500/T}\ m^3/kmole\ sec$	67, 68, 69
$CH_2O + h\nu \rightarrow CO + H_2$	†$1.65 \times 10^{-4}\ e^{-0.48/\cos\theta}\ sec^{-1}$	70
$CH_2O + h\nu \rightarrow CHO + H$	†$6.42 \times 10^{-5}\ e^{-0.48/\cos\theta}\ sec^{-1}$	70
$CH_2O + OH \rightarrow CHO + H_2O$	$4.6 \times 10^{10}\ e^{-460/T}\ m^3/kmole\ sec$	64, 65, 67
$CO + O + M_{14} \rightarrow CO_2 + M_{14}$	$3.6 \times 10^{11}\ e^{-1750/T}\ m^6/kmole^2\ sec$	2, 65
$CO + OH \rightarrow CO_2 + H$	$3.1 \times 10^8\ e^{-300/T}\ m^3/kmole\ sec$	67
$CO + N_2O \xrightarrow{Surface} CO_2 + N_2$	$24.\ e^{-6000/T}\ sec^{-1}$	2

†Exponential term approximates the dependence of the reaction rate on the solar zenith angle. During the night, the exponential term was set to zero so that the photochemical reaction rates were zero.

approximation is used. The parameteric data assumed for the other species are listed in Table II.

The simplified reaction kinetic model was evaluated under static conditions to determine if it was generally consistent with the conclusions of other investigators. The reaction model was evaluated using CSMP on the IBM 370/165 system at the University of Kentucky. The Runge-Kutta fourth order variable step size integration routine was used. The temperature was specified to be 288°K and the water vapor concentration corresponded to approximately 35% relative humidity. The ozone mixing ratio was 0.02 ppm.

The following five features of the reaction kinetic model were investigated: (a) analysis and validity of the pseudo-steady state approximation; (b) extension of the pseudo-steady state approximation to include formaldehyde; (c) the chemical half lives of CH_4 and CO; (d) the non-chemical source strengths of CH_4 and CO requisite with reasonable steady state concentrations of CH_4 and CO; and (e) the homogeneous chemical source strength of CO by gas phase oxidation of methane. Each of these will be discussed separately.

Pseudo-Steady State Approximation

It is virtually impossible due to computation time limiations to rigorously test the pseudo-steady state approximation by integrating the system of differential equations for total time periods on the order of 10^8 seconds using a time step sufficiently small to ensure numerical stability and accuracy. However, an indirect validation can be achieved

TABLE II

Additional Parameter Values Employed in Model

Parameter	Assumed Value	Reference
Temperature	[†]288°K	
Pressure	[†]1 atmosphere	
Solar Zenith Angle	[†]43°	
O_3	0.02 ppm $(8.4 \times 10^{-10}$ kmoles/m^3 at 1 atmosphere and 288°K)	
H_2O	[†]2.5×10^{-4} kmoles/m^3	
M_3	[†]Molar density of air 0.042 kmoles/m^3	2, 64
M_4	[†]Molar density of air 0.042 kmoles/m^3	65
M_{14}	[†]Molar density of air 0.042 kmoles/m^3	65

[†]These parameters were assumed constant in the static model, but were variable in the dynamic transport/chemistry model.

by evaluating the time required for the species to reach a relatively
stable value and also to establish if this stable value corresponds to
that determined when the pseudo-steady state approximation is employed.

Several of the intermediate species were tested in this manner
using the complete reaction mechanism without exploiting the pseudo-steady
state approximation. Transport of the species was not important for
this evaluation. The system of equations was integrated by evaluating
the time step required to ensure numerical stability. In the initial
stages, the time step was specified to be 10^{-10} seconds. When a species
reached at least 95% of its pseudo-steady state value, the pseudo-steady
state approximation was assumed for that species. In this manner, the
time step could be increased slightly. All intermediate species were
not tested since the computer time required would be impractical.
However, sufficient data were obtained to rather conclusively show
that the pseudo-steady state approximation is valid for this system.
In Table III are listed the steady state values for the prescribed
conditions and the time to reach 95% of the steady state value for
three of the species. In the computer simulation, none of the species'
concentration exceeded the pseudo-steady state value. In addition,
even those species that did not reach steady state in the allotted
time appeared to be approaching the steady state value. Finally, it
should be noted that the methane, formaldehyde, and carbon monoxide
concentrations did not change during this time period. With this
evidence, it is felt that the pseudo-steady state approximation is

TABLE III

Test of Pseudo-Steady State Approximation

Species	Steady State Value	Time to Reach 95% of Steady State Value
CH_3O	2.44×10^{-25} kmoles/m^3	
$O^1(D)$	2.21×10^{-24} kmoles/m^3	1.43×10^{-9} sec
CH_3	5.81×10^{-24} kmoles/m^3	
CHO	1.61×10^{-22} kmoles/m^3	4.05×10^{-8} sec
O	6.70×10^{-20} kmoles/m^3	4.51×10^{-5} sec
CH_3O_2	5.11×10^{-18} kmoles/m^3	
OH	7.10×10^{-17} kmoles/m^3	

a valid modeling concept for this reaction scheme.

Pseudo-Steady State Approximation for Formaldehyde

With the success using the pseudo-steady state approximation for the intermediate species, this concept was also tested for formaldehyde since this species was not one of our principal interests. Long term integrations using integration time steps as large as 8.64×10^3 seconds were made to compare the systems in which the pseudo-steady state approximation was either employed or not employed for the formaldehyde. Integrations for periods of 4.75 years showed differences in the concentrations of less than 1%. In addition, the severity of numerical stability problems as evidenced by the required integration time step was much less when pseudo-steady state was assumed for formaldehyde. The reason for this is that even the three differential equations written for CH_4, CH_2O, and CO represent a stiff system, CH_2O being the stiff variable. If the initial condition for CH_2O does not closely correspond to the pseudo-steady state value consistent with the methane and carbon monoxide initial concentrations, small time steps must be used until the formaldehyde can adjust. On the other hand, this stiffness problem is circumvented if the pseudo-steady state approximation is employed for formaldehyde. Certainly one can not obtain the short term initial transient behavior (less than ten days or so) of formaldehyde if the pseudo-steady state approximation is used, but the long term behavior is consistent with the transient model.

Chemical Half Lives.

The chemical half lives must be at least as long as the estimated overall half lives of CH_4 and CO so that inordinately high conversion rates are not simulated. There are various estimates for the overall residence times of methane and carbon monoxide. However, values of 2 - 3 years and 2 - 3 months, respectively, are not unlikely. For the purpose of testing this aspect of the chemical kinetic model, long term simulations up to 4000 days were conducted employing the pseudo-steady state approximation for all the species except methane and carbon monoxide.

The results of those simulations are shown in Figure 3. The initial CH_4 concentration was 6.3×10^{-8} kmoles/m^3 (1.5 ppm mixing ratio), and the initial CO concentration was 4.2×10^{-9} kmoles/m^3 (0.1 ppm mixing ratio). The corresponding chemical half lives were 5.8 years and 1.1 years for the CH_4 and CO, respectively. These values are reasonable when one considers that sinks other than chemical reactions are also operating.

Source Strengths of CH_4 and CO

If the troposphere can be considered a well mixed system, one can obtain estimates of the non-chemical reaction source strengths consistent with the chemical kinetic mechanism. This can be accomplished by adding homogeneous sources of methane and carbon monoxide to Equations (22) and (24), respectively, to account for all other sources of
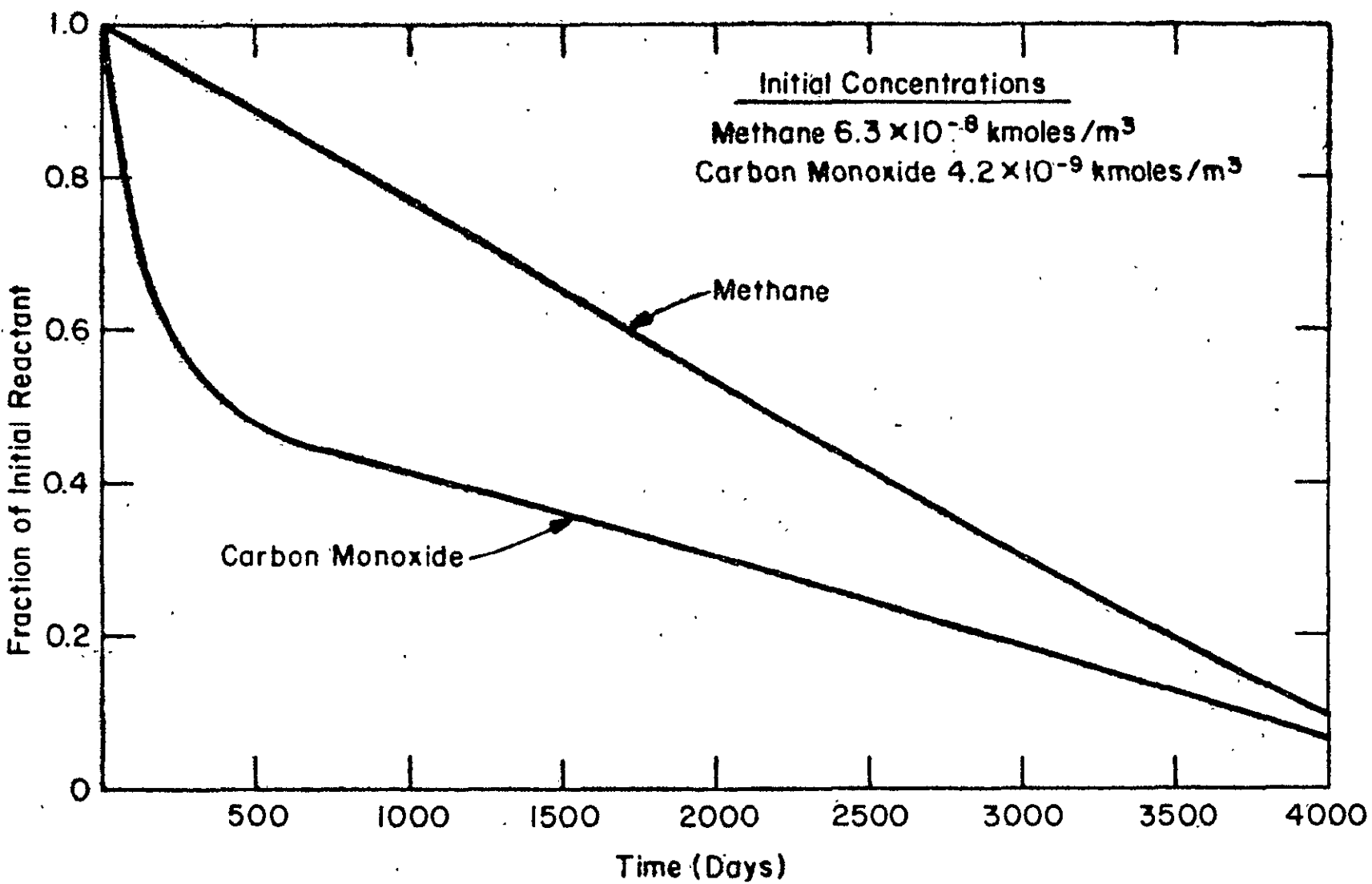
Figure 3

Simulation for Half Life Analysis of Reaction Model

these species. Then the magnitude of these source strengths is that which is consistent with steady state concentrations of CH_4 and CO that one expects in the troposphere. The tropospherically averaged concentrations of CH_4 and CO are approximately 6.3×10^{-8} kmoles/m^3 (1.5 ppm mixing ratio at 288°K) and 4.2×10^{-9} kmoles/m^3 (0.1 ppm mixing ratio at 288°K). In Figure 4, the results of long term simulations where the homogeneous source strengths were fixed at 1.3×10^{-16} kmoles CH_4/m^3 -sec (320×10^6 tons CH_4/year) and 1.5×10^{-16} kmoles CO/m^3 sec (650×10^6 tons CO/year) are shown. It is observed that with these values of the source strengths, the concentrations remain very nearly 1.5 ppm and 0.1 ppm mixing ratio throughout the long term simulation. These source strengths would be changed slightly by assuming a different temperature and/or mixing ratio representative of the troposphere. However, these values are characteristic of the general magnitude that one anticipates for the source strengths of CH_4 and the non-chemical reaction source strength of CO.

CO Source Strength by Methane Oxidation

An estimate for the source strength of carbon monoxide by the gas phase oxidation of methane can also be obtained. One procedure is by recognizing that, according to the simplified reaction scheme, all methane must ultimately be reacted to carbon monoxide. Thus, presuming typical methane and carbon monoxide concentrations and presuming that the formaldehyde concentration can be specified by the pseudo-steady
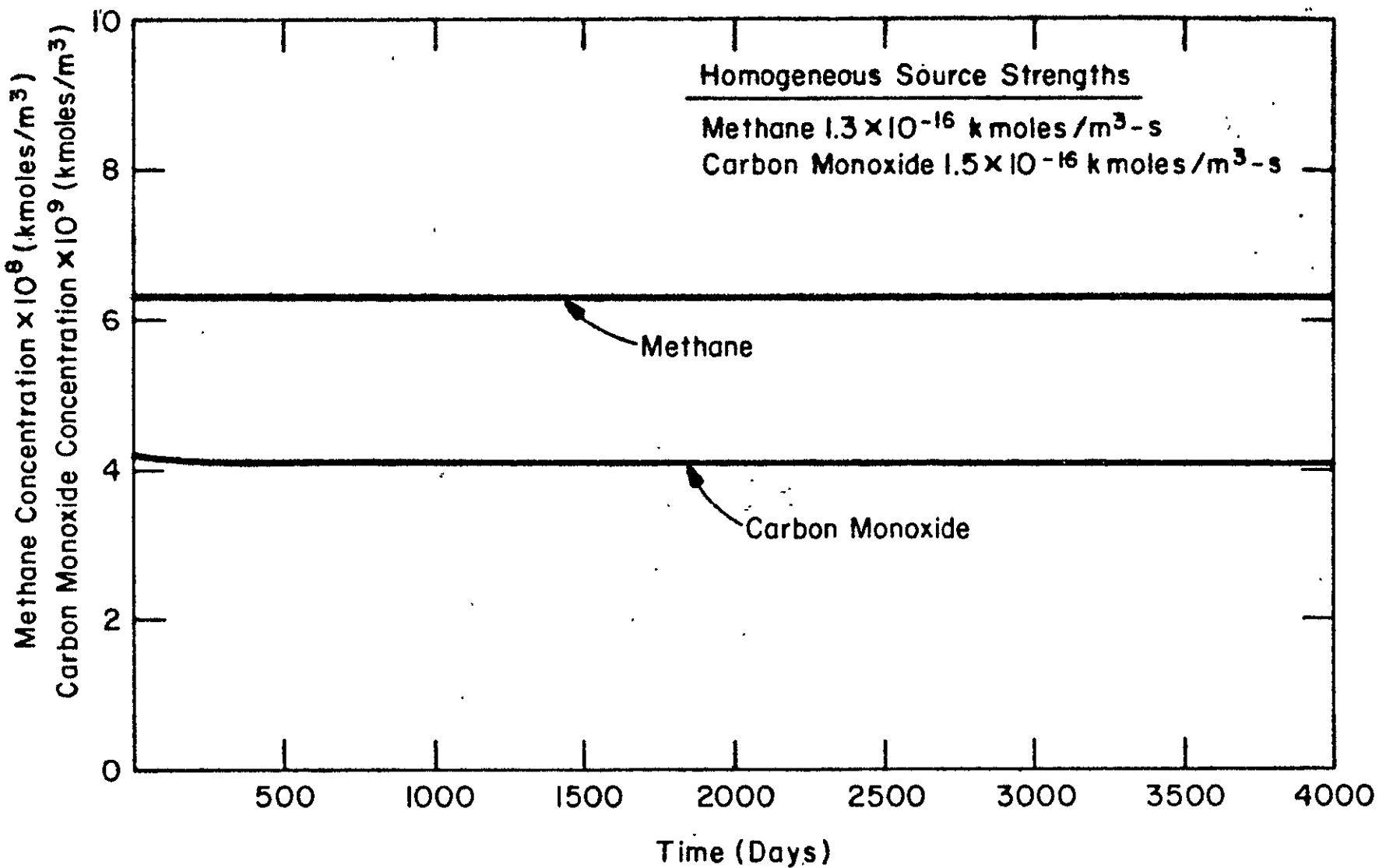
Figure 4

Simulation for Source Strengths of Methane and Carbon Monoxide

state approximation, then the chemical source strength of CO determined by Equation (22) is 1.3×10^{-16} kmoles/m^3-sec. This corresponds to approximately 560×10^6 tons CO/yr which is in reasonable agreement with other estimates. One can also note that at steady state, the homogeneous source of CH_4 is totally converted to CO. As mentioned above, 1.3×10^{-16} kmoles CH_4/m^3 sec is also the best estimate and is in agreement with other work.

Based on all of these evaluations, it can be stated that the simplified mechanism in combination with the pseudo-steady state approximation for all intermediates affords a plausible description of the CH_4 - CO chemistry. With these significant simplifications the combined chemistry/transport model becomes much less time consuming on the computer. As a result of the pseudo-steady state approximation, it is only necessary to solve two species continuity equations.

SIMULATIONS OF DYNAMIC TRANSPORT/CHEMISTRY MODEL

The general approach in the simulation of the global transport/ chemistry model for the CH_4-CO cycle consisted of the following steps:

a. Initialize the CH_4 and CO concentrations in the troposphere. In order to conserve computer time, the initial concentrations selected were approximately that expected in the atmosphere. This would not affect the final results but simply the computer time required to reach some regularly varying atmospheric state relative to the two species concentrations.

b. Distribute the sources and sinks of the various species on
the Earth's surface and at the tropopause consistent with the
physico-chemical considerations. This involved proper inter-
pretation of oceans and lands as sources and/or sinks of the
particular species. As a first approximation, the tropopause
has been considered as a zero flux boundary. Thus, all
pollutant generation and consumption is entirely within the
troposphere.

c. Solve the coupled unsteady state turbulent diffusion
equations for CH_4 and CO with the boundary conditions
established by b. Climatological data were used to estab-
lish the wind field, temperature field, and water vapor
field. The coupling of the diffusion equations, of course,
resulted from the gas phase reactions creating homogeneous
generation terms. This, therefore, accounted for the chem-
ical sources and sinks present.

d. Continue the integration in time

The inherent advantage to using this procedure is that one does
not presuppose the atmospheric concentrations of the three pollutant
species being studied. This, therefore, provides a meaningful test
of the distribution of sources and sinks. This should not imply,
however, that there are not uncertainties present. But these uncer-
tainties are mostly associated with the strengths of the sources and

'sinks, and a primary goal of the current research is to establish good

estimates of these source and sink strengths.

Model Parameters

The basis for the model parameters was January climatological data

obtained from the National Weather Records Center[71, 72]. This

included the horizontal wind field, temperature, and dew point at the

surface, and the same data plus heights at pressure surfaces of 850, 700,

500, 300, 200, and 100 mb. Dew points were available only through the

500 mb surface. The computer model was not restricted to use of this

climatology data. For example, the wind field could just as easily

have been specified by a general circulation model.

Since the global pollution transport model employed geometric

height as the vertical independent variable rather than pressure,

the data were converted to geometric altitude by linear interpola-

tion. The vertical velocity was obtained from the horizontal wind

field using the continuity equation.

The chemical reaction rate constants were based on the tempera-

ture field for those constants that showed a substantial temperature

dependence and are listed in Table I in the preceding section. The

chemical reaction model also required water vapor and ozone concen-

trations as input. The water vapor concentration was established

from the dew point data where possible. At levels of 5 km, 7.5 km,

and 10 km, the water vapor concentration was assumed to be 2.4×10^{-5}

$kmoles/m^3$, 7.2×10^{-6} $kmoles/m^3$, and 1.7×10^{-6} $kmoles/m^3$, in general

agreement with the U.S. Standard Atmosphere. The ozone mixing ratio was assumed to be constant at 0.02 ppm (v/v).

The land and ocean areas were differentiated according to pollution source strength functions and their capacity to exchange the gaseous pollutants with the air. Since the oceans apparently act as sources of both CH_4 and CO, those locations assumed a supersaturation so as to describe the source. For methane, supersaturation corresponded to 1.8 ppm for ocean areas and 1.0 ppm for land areas, whereas for carbon monoxide, these values were 3.5 ppm and 0.2 ppm, respectively. In those grids that had both ocean and land areas, a weighted average corresponding to the fraction of ocean and land area was used. Due to the limited knowledge of gas species interaction with the various soil types, there was no differentiation according to the type of land area. For example, desert areas were considered the same as forested regions in this initial simulation. Since the absorption coefficient, K, is dependent on the Henry's Law constant which varies with temperature, the absorption coefficient for CH_4 and CO were latitude dependent. The basis for the variation of H were zonally averaged sea surface temperatures for January[73]. The absorption coefficient was the same for land and ocean areas at the same latitude.

The anthropogenic sources were approximately prorated according to the degree of urbanization. Therefore, the major amount of these sources were in the Northern Hemisphere.

It was necessary to consider the position of the sun to account for the photochemical reaction rate constants and the apparent diurnal nature of the supersaturation of CO in the oceans. The declination angle was set at $-20°$ consistent with about mid-January, and the initial time for the integration corresponded to 12:00 Greenwich mean time.

Short Term Simulations

Only one other simulation of this type appears to have been performed. Kwok, Langlois and Ellefsen[74] used a general circulation model and incorporated only anthropogenic, source estimates, with the atmosphere initially free of CO. In addition, their simulations did not include any possibility for homogeneous conversion of CH_4 to CO. The present model has attempted to overcome these limitations.

At the present, only short term simulations have been performed, and longer term simulations are required. Typical results are shown in Figures 5 and 6. One of the important features, that of chaining of the isopleths due to the dominant westerly wind field, can be observed being formed. Kwok, Langlois, and Ellefsen[74] also noted this with their CO transport model.

Longer term simulations are being planned at this time. From those simulations, features such as the rate of interhemispheric transport, ground level source strengths, and the homogeneous conversion rate of CH_4 to CO can be evaluated. These statistics will be used to validate and further refine the model.
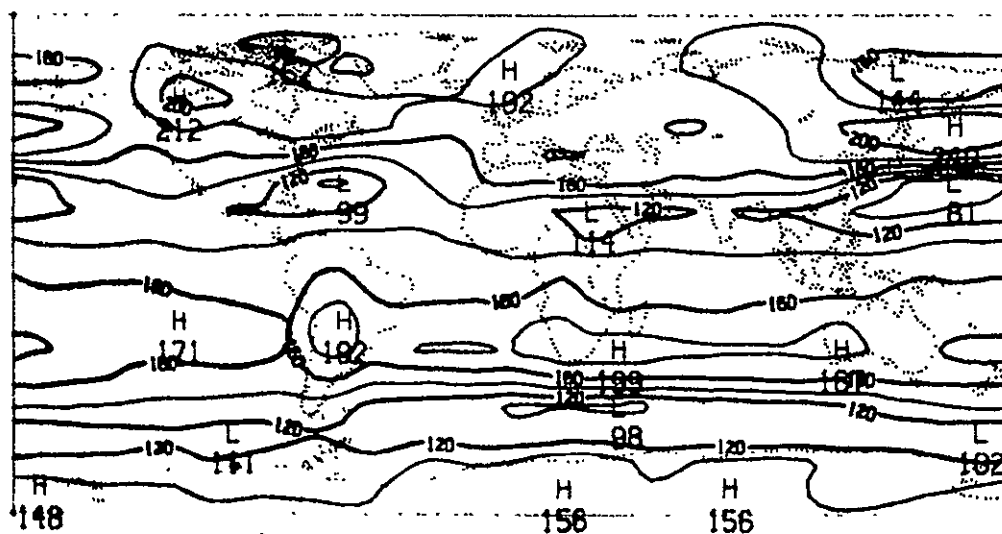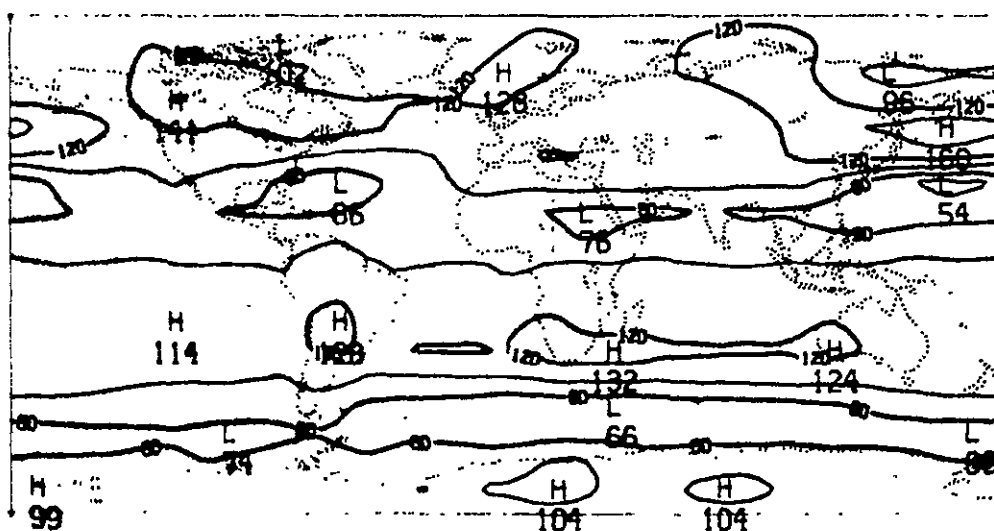
METHANE

TIME = 1.25 DAYS   LEVEL = 6250 METERS

Figure 5

Dynamic transport/chemistry model simulation of methane
concentration. Units on isopleths are ppm x 10^2.

CARBON MONOXIDE

TIME = 1.25 DAYS   LEVEL = 6250 METERS

Figure 6

Dynamic transport/chemistry model simulation of carbon
monoxide concentration.   Units on isopleths are ppm x 10^3.

REFERENCES

1. McCormac, B. M., Editor: Introduction to the Scientific Study of Atmospheric Pollution. D. Reidel Publishing Co., Dordrecht, Holland, 1971.

2. Bortner, M. H., Kummler, R. H., and Jaffe, L. S.: A Review of Carbon Monoxide Sources, Sinks, and Concentrations in the Earth's Atmosphere: NASA CR - 2081, June 1972.

3. Robinson, E. and Robbins, R. C.: Final Report on SRI Project PR 6755, February 1967.

4. Junge, C., Seiler, W., and Warneck, P.: The Atmospheric ^{12}CO and ^{14}CO Budget. J. Geophys. Res., Vol. 76 (1971) pp. 2866 - 2879.

5. Weinstock, B.: Carbon Monoxide Residence Time in the Atmosphere. Science, Vol. 166 (1969) pp. 224 - 225.

6. Wofsy, S. C., McConnell, J. C., and McElroy, M. B.: "Atmospheric CH_4, CO, and CO_2" in Sources, Sinks, and Concentrations of Carbon Monoxide and Methane in the Earth's Environment. Joint Meeting of The American Geophysical Union and The American Meteorological Society; August 1972.

7. Lamontagne, R. A., Swinnerton, J. W., Linnenbom, V. J., and Smith, W.: "Methane Concentrations in Various Marine Environments" in Sources, Sinks, and Concentrations of Carbon Monoxide and Methane in the Earth's Environment. Joint Meeting of The American Geophysical Union and The American Meteorological Society; August 1972.

8. Brooks, J. M. and Sackett, W. M.: "Light Hydrocarbon Concentrations in the Gulf of Mexico" in Sources, Sinks, and Concentrations of Carbon Monoxide and Methane in the Earth's Environment. Joint Meeting of The American Geophysical Union and The American Meteorological Society; August 1972.

9. Levy, H.: Normal Atmosphere: Large Radical and Formaldhyde Concentrations Predicted. Science, Vol. 173 (1971) pp. 141 - 143.

10. Levy, H.: "The Tropospheric Budgets for Methane, Carbon Monoxide, and Related Species" in Sources, Sinks, and Concentrations of Carbon Monoxide and Methane in the Earth's Environment. Joint Meeting of The American Geophysical Union and The American Meteorological Society, August 1972.

11. McConnell, J. C., McElroy, M. B., and Wofsy, S. C.: Natural Sources of Atmospheric CO. Nature, Vol. 223 (1971) pp. 187 - 188.

12. Seiler, W.: The Cycle of Atmospheric CO. <u>Tellus</u>, Vol. 26 (1974) pp. 116 - 135.

13. Seiler, W. and Junge, C.: Carbon Monoxide in the Atmosphere. <u>J. Geophys. Res.</u>, Vol. 75 (1970) pp. 2217 - 2226.

14. Swinnerton, J. W., Linnenbom, V. J., and Check, C. H.: A Sensitive Gas Chromatographic Method for Determining Carbon Monoxide in Sea Water. <u>Limnol. Oceanogr.</u>, Vol. 13 (1968) pp. 193 - 195.

15. Lamontagne, R. A., Swinnerton, J. W., and Linnenbom, V. J.: Non-equilibrium of Carbon Monoxide and Methane at the Air - Sea Interface. <u>J. Geophys. Res.</u>, Vol. 76 (1971) pp. 5117 - 5121.

16. Swinnerton, J. W. and Lamontage, R. A.: Carbon Monoxide in the South Pacific Ocean. <u>Tellus</u>, Vol. 26 (1974) pp. 136 - 142.

17. Meadows, R. W. and Spedding, D. J.: The Solubility of Very Low Concentrations of Carbon Monoxide in Aqueous Solution. <u>Tellus</u>, Vol. 26 (1974) pp. 143 - 150.

18. Rossano. A. T., Jr., Editor: <u>Air Pollution Control Guidebook for Management</u>, Environmental Sciences Services Divisions, 1969.

19. Weinstock, B. and Chang, T. Y.: The Global Balance of Carbon Monoxide. <u>Tellus</u>, Vol. 26 (1974) pp. 108 - 115.

20. Newell, R. E., Boer, G. J., and Kidson, J. W.: An Estimate of the Interhemispheric Transfer of Carbon Monoxide from Tropical General Circulation Data. <u>Tellus</u>, Vol. 26 (1974) pp. 101 - 107.

21. Madley, D. G., and Strickland - Constable, R. F.: <u>Trans. Faraday Soc.</u>, Vol. 34 (1953) p. 1312.

22. Smith, R. N. and Mooi, J.: The Catalytic Oxidation of Carbon Monoxide by Nitrous Oxide on Carbon Surfaces. <u>J. Phys. Chem.</u>, Vol. 59 (1955) pp. 814 - 819.

23. Strickland - Constable, R. F.: <u>Trans. Faraday Soc.</u>, Vol. 34 (1938) p. 137.

24. Bawn, C. E. H.: <u>Trans. Faraday Soc.</u>, Vol. 31 (1936) p. 461.

25. Krause, A.: <u>Bull. Acad. Polon. Sci. Chim.</u>, Vol. 9 (1961) p. 5.

26. Westenburg, A. A.: "The Role of the CO - HO_2 Reaction in the Atmospheric CO Sink" in <u>Sources, Sinks, and Concentrations of Carbon Monoxide and Methane in the Earth's Environment</u>. Joint Meeting of The American Geophysical Union and The American Meteorological Society; August 1972.

27. Davis, D. D., Wong, W., Payne, W. A., and Stief, L. J.: "A Kinetics Study to Determine the Importance of HO$_2$ in Atmospheric Chemical Dynamics: Reaction with CO" in Sources, Sinks, and Concentrations of Carbon Monoxide and Methane in the Earth's Environment. Joint Meeting of The American Geophysical Union and The American Meteorological Society; August 1972.

28. Inman, R. E.: Automotive Air Pollution Research Symposium; Chicago, Illinois; May 1971.

29. Liebl, K. H.,: "The Soil as a Sink and Source for Atmospheric CO. Master's Degree Thesis," Max-Planck-Institut and University of Mainz, Germany (discussed in Ref. 12).

30. Inman, R. E., Ingersoll, R. B., and Levy, E. A.: Science, Vol. 172 (1971) p. 1229.

31. Ingersoll, R. B. and Inman, R. E.: "Soil as a Sink for Atmospheric Carbon Monoxide" in Sources, Sinks, and Concentrations of Carbon Monoxide and Methane in the Earth's Environment. Joint Meeting of The American Geophysical Union and The American Meteorological Society; August 1972.

32. Ingersoll, R. B., Inman, R. E., and Fisher, W. R.: Soil's Potential as a Sink for Atmospheric Carbon Monoxide. Tellus, Vol. 26 (1974) pp. 151 - 159.

33. Schenellen, C.: Doctoral Thesis, Delft, Rotterdam, 1947 (Cited in Reference 2).

34. Goldman, A. Murcray, D. G., Murcray, F. H., Williams, W. J., Brooks, J. N., Bradford, C. M.: "Vertical Distribution of CO in the Atmosphere" in Sources, Sinks, and Concentrations of Carbon Monoxide and Methane in the Earth's Environment. Joint Meeting of The American Geophysical Union and The American Meteorological Society; August 1972.

35. Ehhalt, D. H. and Heidt, L. E.: "Vertical Profiles of CH$_4$ in the Troposphere and Stratosphere" in Sources, Sinks, and Concentrations of Carbon Monoxide and Methane in the Earth's Environment. Joint Meeting of The American Geophysical Union and The American Meteorological Society; August 1972.

36. Ackerman, M. and Muller, C.: "Stratospheric Methane from Infrared Spectra" in Sources, Sinks, and Concentrations of Carbon Monoxide and Methane in the Earth's Environment. Joint Meeting of The American Geophysical Union and The American Meteorological Society; August 1972.

37. Bird, R. B., Stewart, W. E., and Lightfoot, E. N.: <u>Transport Phenomena</u>. John Wiley and Sons, Inc., New York, 1960.

38. Willoughby, R. A., Editor, <u>Stiff Differential Systems</u>. Plenum Press, New York, 1974.

39. Gear, C. W., "Automatic Integration of Stiff Ordinary Differential Equations," Proceedings of IFIP Congress, Supplement, Booklet A, 81, 1968.

40. Lapidus, L., Aiken, R. C., and Liu, Y. A., in Willoughby, Ralph A., Editor, <u>Stiff Differential Systems</u>, Plenum Press, New York (1974) p. 187 - 200.

41. Okubo, A.: "Horizontal and Vertical Mixing in the Sea," D. W. Hood, Editor, <u>Impingement of Man on the Oceans</u>; Wiley - Interscience, New York (1971) p. 141.

42. Broecker, W. S., Li, Y. H., and Peng, T. H.: "Carbon Dioxide-Man's Unseen Artifact," D. W. Hood, Editor, <u>Impingement of Man on the Oceans</u>; Wiley - Interscience, New York (1971) pp. 287 - 324.

43. Seiler, W. and Warneck, P.: Decrease of Carbon Monoxide Mixing Ratio at the Tropopause. <u>J. Geophys. Res.</u>, Vol. 77 (1972) pp. 3204 - 3214.

44. Machta, L.: "Sources and Sinks from Profile Data" in <u>Sources, Sinks, and Concentrations of Carbon Monoxide and Methane in the Earth's Environment</u>. Joint Meeting of The American Geophysical Union and The American Meteorological Society; August 1972.

45. Arakawa, A.: Computational Design for Long - Term Numerical Integration of the Equations of Fluid Motion: Two - Dimensional Incompressible Flow, Part I. <u>J. Computat. Phys.</u>, Vol. 1 (1966) pp. 119 - 143.

46. Roberts, K. V. and Weiss, N. O.: Convective Difference Schemes. <u>Math. of Computat.</u>, Vol. 20 (1966) pp. 272 - 299.

47. Lilly, D. K.: On the Computational Stability of Numerical Solutions of Time Dependent Non-Linear Geophysical Fluid Dynamics Problems. <u>Monthly Weather Review</u>, Vol. 93 (1965) pp. 11 - 26.

48. Harlow, F. H. and Nakayama, P. I.: Turbulence Transport Equations. <u>Phys. Fluids</u>, Vol. 10 (1967) pp. 2323 -2332.

49. Leith, C. E.: "Numerical Simulation of Turbulent Flow," <u>Properties of Matter Under Unusual Conditions</u>; Editors, H. Mark and S. Fernbach, Inter-Science Publishers, New York (1969) pp. 267 - 271.

50. Gowain, T. H. and Pritchett, J. W.: A Unified Heuristic Model of Turbulence. J. Computat. Phys., Vol. 5 (1970) pp. 383 - 405.

51. Deardorff, J. W.: A Numerical Study of Three Dimensional Turbulent Channel Flow at Large Reynolds Numbers. J. Fluid Mech., Vol. 41, Part 2 (1970) pp. 453 - 480.

52. Crowley, W. P.: Second - Order Numerical Advection. J. Computat. Phys., Vol. 1 (1966) pp. 471 - 484.

53. Fromm, J. E.: A Method for Reducing Dispersion in Convective Difference Schemes. J. Computat. Phys., Vol. 3 (1968) pp. 176 - 189.

54. Fromm, J. E.: Practical Investigation of Convective Difference Approximations of Reduced Dispersion. Phys. Fluids, Supplement II, Vol. 12 (1969) pp. II - 3 - II - 12.

55. Orszag, S. A.: Numerical Methods for the Simulation of Turbulence. Phys. Fluids, Supplement II, Vol. 12 (1969) pp. II - 250 - II - 257.

56. Boris, J. P. and Book, D. L.: Flux - Corrected Transport, J. Computat. Phys., Vol. 11 (1973) pp. 38 - 69.

57. Smagorinsky, J., Manabe, S., and Holloway, J. L., Numerical Results From a Nine - Level General Circulation Model of the Atmosphere. Monthly Weather Review, Vol. 93 (1965) pp. 727 - 768.

58. Leith, C. E.: Diffusion Approximation for Two - Dimensional Turbulence. Phys. Fluids, Vol. 11 (1968) pp. 671 - 673.

59. Leith, C. E.: Two - Dimensional Eddy Viscosity Coefficients. Proceedings of the WMO/IUGG Sumposium on Numerical Weather Prediction, Tokoyo (1968) pp. I - 41 - I - 44.

60. Monin, A. S. and Zilitinkevich, S. S.: On Description of Micro - and Meso - Scale Phenomena in Numerical Models of the Atmosphere. Proceedings of the WMO/IUGG Symposium on Numerical Weather Prediction, Tokyo (1968) pp. I - 105 - I - 122.

61. Crowley, W. P.: A Numerical Model for Viscous, Free - Surface, Barotropic Wind Driven Ocean Circulations. J. Computat. Phys., Vol. 5 (1970) pp. 139 - 168.

62. Manabe, S., Smagorinsky, J., Holloway, J. L., and Stone, H. M.: Simulated Climatology of a General Circulation Model with a Hydrologic Cycle. Monthly Weather Review, Vol. 98 (1970) pp. 175 - 213.

63. Kummler, R. H., Bortner, M. H., and Baurer, T.: The Hartley Photolysis of Ozone as a Source of Singlet Oxygen in Polluted Atmospheres. _Environ. Sci. Tech._, Vol. 3 (1969) pp. 248 - 250.

64. Kummler, R. H. and Baurer, T.: A Temporal Model of Tropospheric Carbon - Hydrogen Chemistry. _J. Geophys. Res._, Vol. 78 (1973) pp. 5306 - 5316.

65. Schofield, K.: An Evaluation of Kinetic Rate Data for Reactions of Neutrals of Atmospheric Interest. _Planet. Space Sci._, Vol. 15 (1967) pp. 643 - 670.

66. Huie, R. E., Herron, J. T., and Davis, D.D.: Absolute Rate Constants for the Reaction $O+O_2+M \rightarrow O_3+M$ Over the Temperature Range 200-346°K. _J. Phys. Chem._, Vol. 76 (1972) pp. 2653 - 2658.

67. Wilson, W. E.: A Critical Review of the Gas Phase Reaction Kinetics of the Hydroxyl Radical. _J. Phys. Chem. Ref. Data_, Vol. 1 (1972) pp. 535 - 573.

68. Dixon - Lewis, G. and Williams, A.: Eleventh International Symposium on Combustion; The Combustion Institute, p. 951, 1967.

69. Baker, R., Baldwin, R., and Walker, R.: Thirteenth International Symposium on Combustion; The Combustion Institute, p. 291, 1971.

70. Calvert, J. G., Kerr, J. A., Demerjian, K. L., and McQuigg, R. D.: Photolysis of Formaldehyde as a Hydrogen Atom Source in the Lower Atmosphere. _Science_, Vol. 175 (1972) pp. 751 - 752.

71. Crutcher, H. L. and Jenne, R. L.: Northern Hemisphere Climatological Grid Data Tape. National Center for Atmospheric Research; July 1969.

72. Jenne, R. L., Crutcher, H. L., Van Loon, H., and Taljaard, J. J.: Southern Hemisphere Climatological Grid Data. National Center for Atmospheric Research; September 1969.

73. Shutz, C. and Gates, W. L.: Supplemental Global Climatic Data: January. Rand Report R-915/1-ARPA; May 1972.

74. Kwok, H. C. W., Langlois, W. E., and Ellefsen, R. A.: Digital Simulation of the Global Transport of Carbon Monoxide. _IBM J. Res. Develop._, Vol. 15 (1971) pp. 3 - 9.